Triazenides as Suitable Ligands in the Synthesis of Palladium Compounds in Three Different Oxidation States: I, II, and III

ARTICLE *in* ORGANOMETALLICS · OCTOBER 2014

Impact Factor: 4.13 · DOI: 10.1021/om500702j

6 AUTHORS, INCLUDING:

Susana Ibáñez
Universitat Jaume I
23 PUBLICATIONS **253** CITATIONS
SEE PROFILE

Francisco Estevan
University of Valencia
57 PUBLICATIONS **711** CITATIONS
SEE PROFILE

ORGANOMETALLICS

Article

pubs.acs.org/Organometallics

Triazenides as Suitable Ligands in the Synthesis of Palladium Compounds in Three Different Oxidation States: I, II, and III

Susana Ibañez,[†] Larisa Oresmaa,[‡] Francisco Estevan,[†] Pipsa Hirva,*[,‡] Mercedes Sanaú,[†] and M[a] Angeles Úbeda*[,†]

[†]Departament de Química Inorgànica, Universitat de València, Dr. Moliner 50, 46100-Burjassot, Valencia, Spain

[‡]Department of Chemistry, University of Eastern Finland, Joensuu Campus, P.O. Box 111, FI-80101 Joensuu, Finland

Supporting Information

ABSTRACT: New orthometalated dinuclear triazenide palladium(II) compounds of the general formula $Pd_2[(C_6H_4)PPh_2]_2[R{-}N{-}N{-}N{-}R]_2$ (R = C_6H_5, **3a**; *o*-BrC_6H_4, *o*-**3b**; *o*-$MeOC_6H_4$, *o*-**3c**; *o*-MeC_6H_4, *o*-**3d** ; *p*-BrC_6H_4, *p*-**3b**; *p*-$MeOC_6H_4$, *p*-**3c**; *p*-MeC_6H_4, *p*-**3d**) have been synthesized and structurally characterized. The characteristics of these compounds were compared with the isoelectronic formamidinate derivatives. These triazenide compounds have been suitable starting products in the synthesis of new not so common dinuclear palladium(I) compounds and new unusual palladium(III) ones. In the presence of an excess of the triazenide ligand, compounds *o*-**3b** and *o*-**3c** underwent a reduction process giving dinuclear palladium(I) compounds, $Pd_2[R{-}N{-}N{-}N{-}R]_2$ (R = *o*-BrC_6H_4, *o*-**4b**; R = *o*-$MeOC_6H_4$, *o*-**4c**). DFT calculations verified the importance of the mostly noncovalent Pd···Br or Pd···OMe axial interactions on the stability of these compounds. Under cyclic voltammetric conditions, compounds **3** with the only exception of compound *o*-**3b**, were found to undergo a first reversible wave that is assigned as the Pd_2^{5+}/Pd_2^{4+} pair. Compounds *p*-**3b**-**d** also showed at more positive potentials a second reversible wave, Pd_2^{5+}/Pd_2^{6+} pair. When the electrochemical oxidation was performed in the presence of chloride, the Cl−Pd(III)−Pd(III)−Cl species were detected. By chemical oxidation of the palladium(II) complexes with $PhICl_2$, two new relatively stable dinuclear palladium(III) compounds, $Pd_2[(C_6H_4)PPh_2]_2[R{-}N{-}N{-}N{-}R]_2Cl_2$ (R = C_6H_5, **5a**; R = *p*-BrC_6H_4, *p*-**5b**), were synthesized and spectroscopically characterized at low temperature. DFT calculations have been performed to study the stability of all the palladium complexes. The isolated palladium(III) and -(II) compounds have been tested as precatalysts at room temperature in the catalytic 2-phenylation of indole with $[Ph_2I]PF_6$. With **3a** the reaction was complete in the shortest reaction time, 7 h, with a 88% isolated yield. The highest yield (99%) but with higher reaction time, 24 h, was obtained with *o*-**3d** when CH_2Cl_2 was added to the reaction medium with the aim of solving the palladium complex. These catalytic results were compared with those obtained with other orthometalated palladium compounds with isoelectronic ligands: formamidinate and carboxylates. In the search for a possible first step in this catalytic oxidation process we have also performed DFT calculations exploring the potential Pd(III) intermediate formed by axial Pd−Ph interactions.

INTRODUCTION

N,N′ donor ligands such as guanidinates, amidinates, and triazenides are versatile ligands in coordination chemistry, but in the case of the triazenes, their use is less developed[1] even though the aryltriazenides have been studied for their interesting structural, anticancer, and reactivity properties.[2]

The aryltriazenide anions are "short-bite" three atoms donor ligands that can act in monodentate, chelating, or bridging coordination modes (Figure 1).[1b,3,4b] The chelating mode is less common for these ligands that exhibit a propensity to coordinate in bridging mode, in part, attributed to the parallel projection of the two N-donor atom orbitals because of the lack of substituents in the central atoms that avoids some steric interferences.[1,3]

The triazenide ligands, even though they are isoelectronic with amidinate ligands, are weaker donors and more amenable to binding to late transition metals.[4] Triazenide ligands are also isoelectronic with carboxylate ones, and the complexes with these bridging ligands exhibit some M−M interactions.[5]

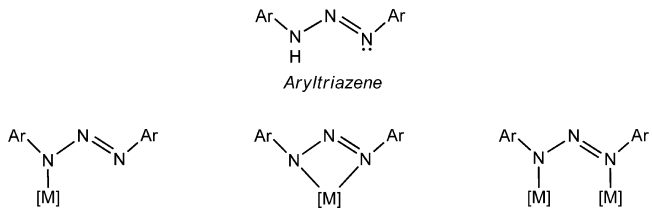

Figure 1. Aryltriazene and the coordination modes of the triazenide ligands.

The palladium triazenide chemistry is scarce, and few of these complexes have been structurally characterized. Both coordination modes, chelating[6] and bridging,[4,7] were observed in the palladium(I)[4] and -(II)[6,7] compounds described in the literature.

Received: July 7, 2014
Published: September 26, 2014

   dx.doi.org/10.1021/om500702j | *Organometallics* 2014, 33, 5378−5391

In the last years our research has focused on the palladium(III) organometallic chemistry, specifically in the dinuclear compounds with Pd_2^{6+} core and M−M bond, being the first that reported the synthesis in high yield of these complexes.[8] This chemistry is nowadays not well-known, and only a few mononuclear and dinuclear compounds have been characterized.[9]

Ritter and co-workers have synthesized and characterized not only other discrete dinuclear palladium(III) complexes[10] but also a transition state analogue for the oxidation of a palladium(II) compound to a palladium(III) one.[11] Furthermore, Mirica and co-workers reported a new cationic dinuclear compound with a delocalized Pd^{III}−X−Pd^{III} electronic structure.[12]

The synthetic accessibility of palladium compounds in high oxidation states (III and IV) carried out in the last years has allowed the development of new strategies in which these compounds are considered as intermediates in oxidation catalytic processes. Sanford and Hickman described the advantages of "high valent" organometallic palladium(III) and -(IV) intermediates over the more common "low valent" analogues.[13] Ritter and co-workers brought forward the first evidence of dinuclear palladium(III) intermediates in Pd-catalyzed C−H oxidation reactions.[10,14] The advantages of dinuclear palladium(III) intermediates versus the mononuclear palladium(IV) ones are based in a possible metal−metal cooperation that can lower the oxidation barriers for the oxidation processes.

The triazenides as bridging ligands have allowed us to study the palladium chemistry on three of its oxidation states: the most common II, the not so common I, and the unusual III. In this paper we present the synthesis and characterization of new orthometalated dinuclear palladium(III) and -(I) compounds (Figure 2 A, B) with the M−M bond that were obtained respectively by oxidation or reduction of the new palladium(II) precursors (Figure 2C).

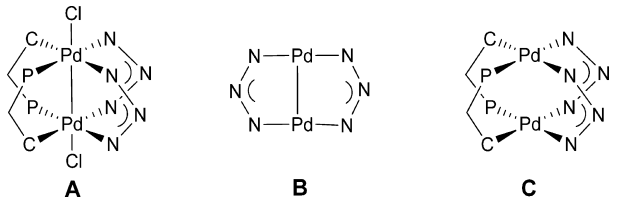

Figure 2. Dinuclear triazenide palladium(III) (**A**), palladium(I) (**B**), and palladium(II) (**C**) compounds.

DFT calculations have been performed for all the palladium-(III) and -(II) compounds to establish results for the geometrical and electronic differences. In addition, the relative stability of the bimetallic Pd(II), Pd(III), and Pd(I) compounds formed in the synthetic reaction steps has been investigated. The results are compared with the previously published for compounds with isoelectronic ligands: formamidinates and carboxylates.[8a,c]

Arylated heteroarenes are compounds with a marked interest because of their optical and electronic properties and their biomedical applications. In their synthesis the direct C−H arylation has emerged as a viable alternative for the traditional cross-coupling reaction, representing an economically and environmentally attractive strategy.[15a,b] Sanford and co-workers reported a new protocol for the direct 2-arylation of free and *N*-substituted indoles and pyrroles catalyzed by the mononuclear palladium(II) compound $IMesPd(O_2CCH_3)_2$ [IMes = 1,3-bis(2,4,6-trimethylphenyl)imidazol-2-ylidene] using hypervalent iodine salts as arylation agents.[15c] The reaction proceeded under very mild conditions, generally at room temperature, and it was completely air/moisture insensitive. The authors proposed a Pd(II)/(IV) pathway in these systems.

In a previous paper, we have studied this catalytic reaction using $[Ph_2I]PF_6$ and orthometalated phenolate and acetylacetonate palladium(II) and -(III) compounds as precatalyts. Some results showed that the reaction was complete in short periods of time with high isolated yields.[8d]

Following the protocol described in the literature, the dinuclear metalated triazenide compounds have been tested in the direct 2-phenylation of the *N*-unprotected indole at room temperature obtaining, in some cases, high isolated yields and short reaction times in the synthesis of 2-phenylindole. Moreover, in the search for the possible first step in this catalytic oxidation process via an Pd(III) intermediate, the interaction of the phenyl groups with the palladium at the axial sites has been studied by DFT calculations.

RESULTS AND DISCUSSION

A. Dinuclear Palladium(II) Compounds with Bridging Triazenide Ligands. *Synthesis and Characterization.* Compounds **3** of the general formula $Pd_2[(C_6H_4)PPh_2]_2[R-N-N-N-R]_2$ were obtained following two different procedures described in Scheme 1

i. Compounds **3a** (R = C_6H_5), *o*-**3b** (R = *o*-BrC_6H_4), *p*-**3b** (R = *p*-BrC_6H_4), and *p*-**3d** (R = *p*-MeC_6H_4) were synthesized by reaction of the tetranuclear palladium(II) compound, **1**, with the corresponding silver triazenide (ratio = 1:4) (Scheme 1a).

ii. Compounds *o*-**3c** (R = *o*-$MeOC_6H_4$), *o*-**3d** (R = *o*-MeC_6H_4), and *p*-**3c** (R = *p*-$MeOC_6H_4$) were also obtained from **1** via the cationic solvated dinuclear compound **2**, by reaction with potassium or sodium triazenides (ratio = 1:4) (Scheme 1b).

The ^{31}P NMR spectra of compounds of type **3** showed a single signal, and their δ (ppm) values are listed in Table 1. Compounds *o*-**3b**−**d** with *ortho*-substituted triazenide ligands in comparison with the *para*- and unsubstituted ones (*p*-**3b**−**d** and **3a**) show δ values shifted toward high fields. It can be considered that this fact is due to axial interactions of the *ortho*-substituents of the phenyl groups in the triazenide ligands with the palladium atoms. The interactions X−Pd (X = Br, MeO) in compounds *o*-**3b** and *o*-**3c** have been studied by DFT calculations in Section E.

Compounds **3a**, *o*-**3b**,**d**, and *p*-**3b**−**d** were structurally characterized by single-crystal X-ray diffraction methods (CCDC 996514-996516, 996518-996520). Figure 3 shows the ORTEP view for compounds *o*-**3b** and *p*-**3b**. Selected bond distances and angles for the six compounds are given in Table 2.

The six compounds show similar paddlewheel structures in which the bimetallic unit is supported by two metalated phosphines and two triazenide ligands, completing the palladium square planar coordination mode. The Pd−Pd distances from 2.6618(9) to 2.7129(9) Å are shorter than the sum of the van der Waals palladium radii (3.26 Å). We have included in this paper a charge density analysis at the Pd−Pd bond critical points (BCPs) that supports a Pd(II)···Pd(II) interaction with some electrons sharing in all the palladium(II) compounds, already observed in previous dinuclear palladium-

dx.doi.org/10.1021/om500702j | *Organometallics* 2014, 33, 5378−5391

Scheme 1. a) and b) Synthesis of Palladium(II) Compounds, $Pd_2[(C_6H_4)PPh_2]_2[R-N-N-N-R]_2$, and c) Synthesis of Palladium(I) Compounds, Pd_2 $[R-N-N-N-R]_2$

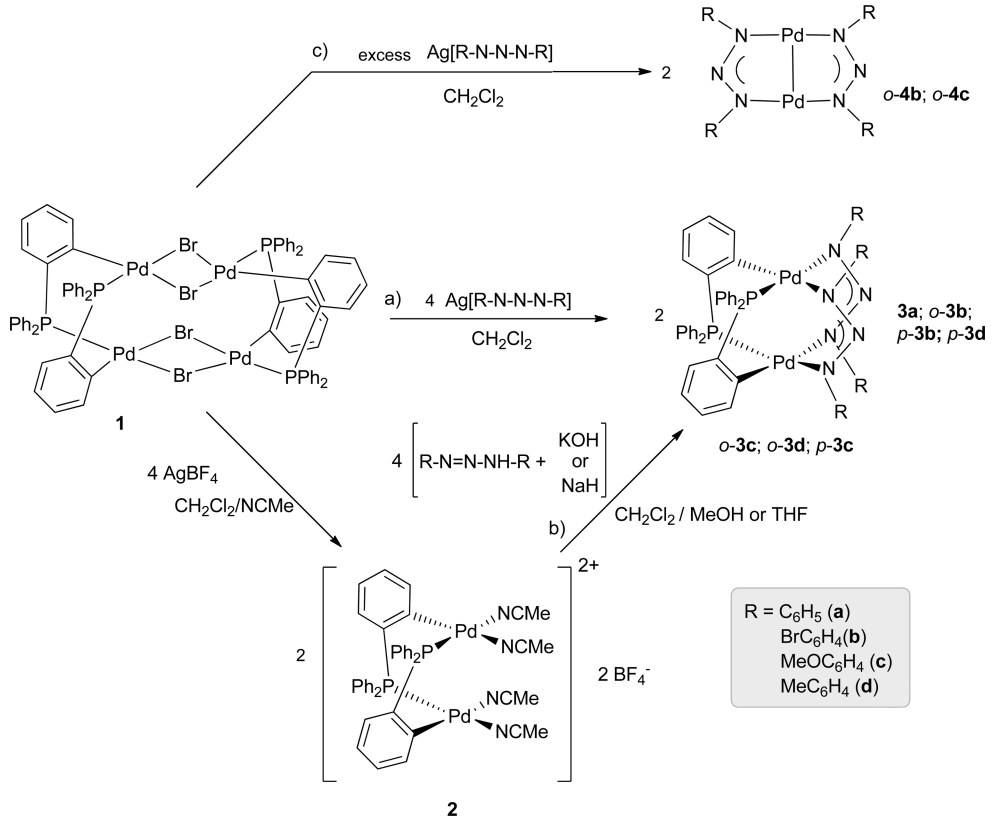

Table 1. ^{31}P NMR Spectroscopy Data at 298 and 200 K for Palladium(II) and -(III) Compounds

palladium(II) compounds			palladium(III) compounds	
compound	δ (ppm) 298 K	δ (ppm) 200 K	compound	δ (ppm) 200 K
3a	3.3	4.4	**5a**	−35.5
o-**3b**	0.7	1.0	*o*-**5b**	
o-**3c**	2.5	3.1	*o*-**5c**	−30.8, −31.0
o-**3d**	−0.3	1.2	*o*-**5d**	−43.5, −48.9, −56.2, −57.1
p-**3b**	3.8	4.3	*p*-**5b**	−34.9
p-**3c**	3.4	4.7	*p*-**5c**	−34.5
p-**3d**	3.4	4.6	*p*-**5d**	−35.3

(II) compounds.[8c,d] The nature of the interaction is not purely electrostatic but a typical metallophilic interaction, as can be seen from the properties of the electron density shown in Table S2, and further discussed in the computational section.

The short Pd···Br distance of 3.0122(9) Å in compound *o*-**3b** supports an axial interaction which results in an increase of the Pd(II)−Pd(II) distance. Compound *o*-**3b** shows the largest distance compared with the compounds without an axial interaction.

The Pd−Pd distances are also shorter than the observed in similar formamidinate dinuclear palladium compounds previously studied and characterized (2.711−2.717 Å) (Table 3).[8c]

Electrochemical Studies. As a previous step in the synthesis of palladium(III) compounds we have carried out studies on the electrochemical behavior of the palladium(II) precursors. Electrochemical oxidation of type **3** compounds was conducted in CH_2Cl_2 solution at room temperature. The cyclic voltammograms are shown in Figures 4, 5, and S1, and the electrochemical potential data versus SCE are summarized in Table 4.

With the exception of *o*-**3b**, all the dinuclear compounds **3** showed one first quasireversible (**3a**, *o*-**3c,d**) or reversible (*p*-**3b−d**) wave that can be described in terms of one-electron transfer process in the starting Pd_2^{4+} complexes yielding the mixed-valent Pd_2^{5+} cationic species.[8,10a,16]

A second reversible wave was observed for compounds with the *para*-substituted phenyl triazenide ligands, *p*-**3b−d**, that was assigned to the Pd_2^{+6}/Pd_2^{+5} couple.

Irreversible oxidation of the triazenes occurs at potentials around 1.5 V (Figure S2).

The comparison of the anodic and cathodic potential values of the first and the second oxidation process among the triazenide and *p*-substituted triazenide compounds (**3a**, *p*-**3b−d**) with the corresponding ones for the equivalent formamidinate $Pd_2[(C_6H_4)PPh_2]_2[R-N-C(H)-N-R]_2$ (R = C_6H_5, *p*-$MeOC_6H_4$, *p*-MeC_6H_4) compounds showed higher potential values in all the triazenide derivatives.[8c] Even though the triazenide ligands are isoelectronic with amidinate ligands these results support the fact that the triazenides are weaker donor ligands.

Since the stability of the species formed in the oxidation could be influenced by the presence of ligands which occupy the axial position, cyclic voltammograms were also performed in the presence of two mols of chloride from tetraethylammonium chloride (TEACl) per one mol of dinuclear palladium(II) compound. In *p*-**3b,d**, the voltammograms of which showed two reversible waves, the addition of chloride changed their electrochemical behavior as it is observed in Figure 5 for

dx.doi.org/10.1021/om500702j | *Organometallics* 2014, 33, 5378−5391

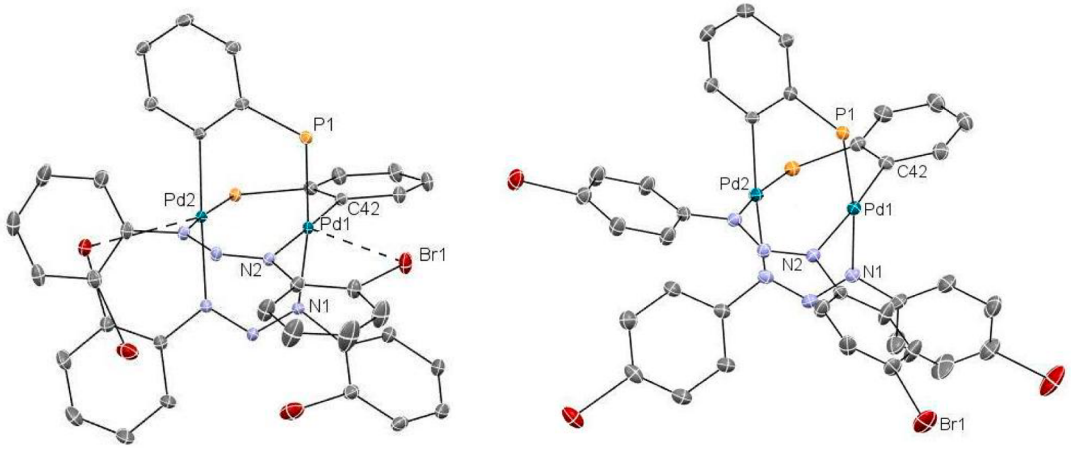

Figure 3. ORTEP view for compounds *o*-**3b** and *p*-**3b**, with the H atoms and the nonmetalated phenyl groups of the phosphines omitted for clarity. Ellipsoids drawn at 25% probability.

Table 2. Selected Distances (Å) and Angles (deg) for Compounds 3a, *o*-3b, *p*-3b, *p*-3c, *o*-3d, and *p*-3d

	compounds					
	3a	***o*-3b**	***p*-3b**	***p*-3c**	***o*-3d**	***p*-3d**
Pd(1)–Pd(2)	2.6771(8)	2.7129(9)	2.6623(6)	2.6794(9)	2.6696(8)	2.6618(9)
Pd(1)–P(1)	2.2743(12)	2.2537(13)	2.2666(16)	2.279(2)	2.2630(19)	2.266(2)
Pd(1)–N(1)	2.099(4)	2.125(4)	2.116(5)	2.115(6)	2.115(6)	2.121(7)
Pd(1)–N(2)	2.178(3)	2.158(4)	2.160(5)	2.145(5)	2.136(5)	2.144(8)
Pd(1)–C(42)	2.010(4)	2.018(4)	2.018(6)	2.007(7)	2.020(7)	2.031(8)
N(1)–Pd(1)–C(42)	88.77(16)	89.76(17)	92.3(2)	90.6(3)	90.5(2)	93.7(3)
N(1)–Pd(1)–N(2)	88.85(15)	89.02(15)	87.2(2)	88.8(2)	87.1(2)	85.4(3)

Table 3. Pd–Pd Distances in Formamidinate Palladium(II) Compounds, $Pd_2[(C_6H_4)PPh_2]_2[R–N–C(H)–N–R]_2$[a]

Pd-Pd distances (Å)	
$Pd_2[(C_6H_4)PPh_2]_2[R\text{-}N\text{-}C(H)\text{-}N\text{-}R]_2$ 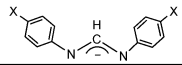	
X = H	2.715
X = OMe	2.771
X = Me	2.717

[a]Reference 8c.

compound *p*-**3b**. When two equivalents of TEACl were added the voltammograms showed one single oxidation anodic wave at a potential slightly lower to the first one recorded for the parent compound. This wave approaches an irreversible two-electron oxidation process followed, in the subsequent cathodic scan, by a reduction wave at 0.35 V and whose anodic counterpart is entirely absent. The anodic and cathodic waves of the starting *p*-**3b** disappeared completely. The electrochemical oxidation involves a two-electron oxidation with addition of two chlorides giving Cl–Pd(III)–Pd(III)–Cl species. The voltammogram of the palladium(III) compound *p*-**5b** with axial Pd–Cl bonds (Figure S3) showed the same anodic wave supporting the formation of this compound by electrochemical reaction of the corresponding palladium(II) compound in the presence of the chloride. Compounds *o*-**3c** (Figure S4), **3a** (Figure S5), and *o*-**3d** with only one reversible wave showed the same behavior. With excess of TEACl an additional wave corresponding to the $Cl^- \rightarrow Cl_2$ oxidation was observed at 1.3 V (Figure S6).

In the case of compound *p*-**3c** the voltammogram registered in the presence of two equivalents of chloride maintains the reversible wave assigned to the Pd_2^{+5}/Pd_2^{+4} couple, but now the second oxidation process is irreversible. No new waves that can be assigned to oxidized species with Cl–Pd interactions were detected (Figure S7). The $Cl^- \rightarrow Cl_2$ oxidation was also observed.

This behavior was already observed in other dinuclear palladium(III) compounds and implies that the oxidation of the dinuclear palladium(II) compound would be followed by the addition of chloride in the axial positions to give Cl–Pd(III)–Pd(III)–Cl species.[16]

B. Dinuclear Palladium(I) Compounds with Bridging Triazenide Ligands. The reaction of **1** with an excess of the silver triazenides with Lewis basic donor substituents in the *ortho* position of their phenyl groups allowed the evolution of *o*-**3b** and *o*-**3c** toward the dinuclear palladium(I) compounds $Pd_2[R–N–N–N–R]_2$ (R = *o*-BrC_6H_4, *o*-**4b**; R = *o*-$MeOC_6H_4$, *o*-**4c**) (Scheme 1c), being quantitative in the case of *o*-**3c**. This procedure involves the Pd(II) → Pd(I) reduction that was also observed by Walsh and co-workers in the reaction of the bis(acetonitrile)palladium(II) dichloride with a mixture of triethylamine and a triazenide with *o*- $MeCO_2$ or *o*-MeO-substituents.[4b]

Suitable crystals for single-crystal X-ray diffraction methods were obtained from the reaction medium. Compound *o*-**4b** could be only structurally characterized (Figure 6) (CCDC 996517), whereas *o*-**4c** had been previously characterized.[4b]

The structure of *o*-**4b** was consistent with those reported by Walsh and co-workers[4c] and Zhan and co-workers[4d,e] with

dx.doi.org/10.1021/om500702j | *Organometallics* 2014, 33, 5378–5391

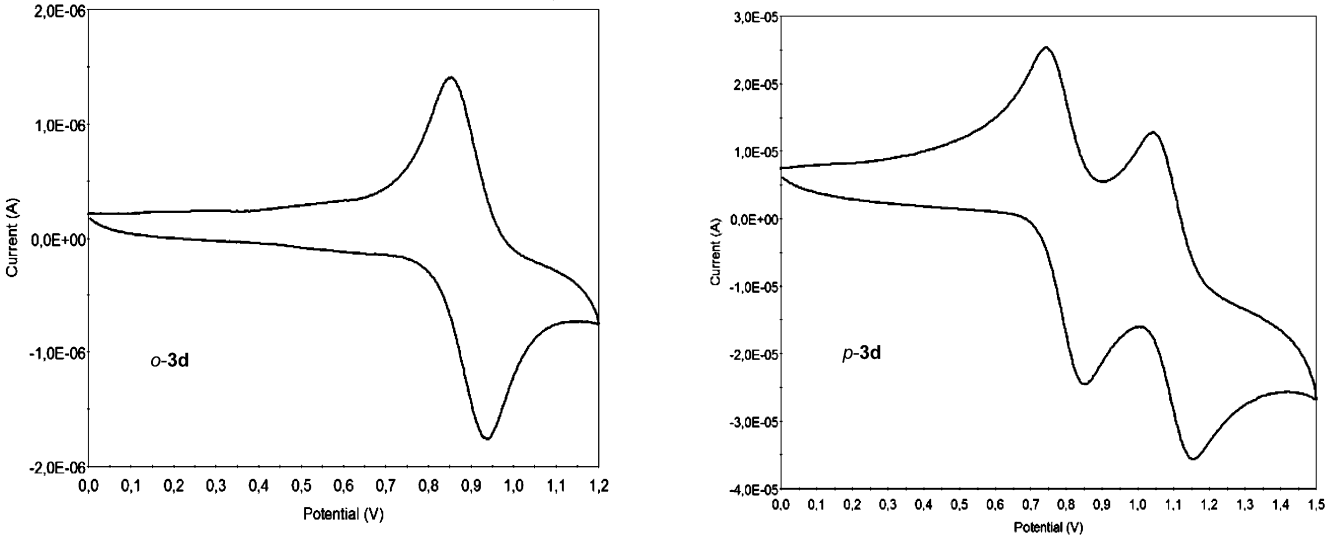

Figure 4. Cyclic voltammograms for compounds *o*-**3d** and *p*-**3d**.

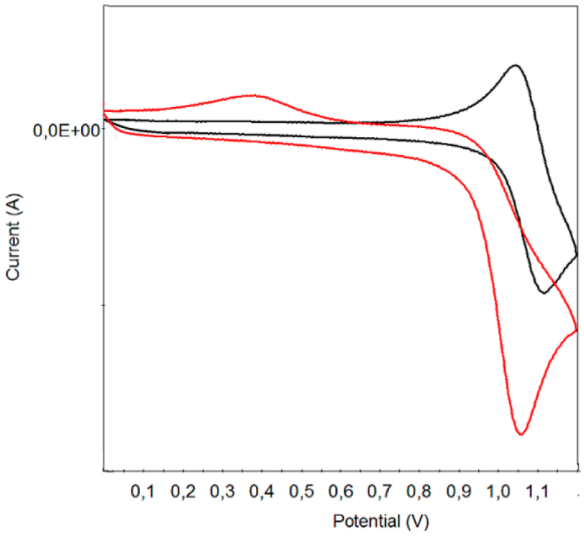

Figure 5. Cyclic voltammogram for compound *p*-**3b** (black). Cyclic voltammogram of *p*-**3b** with two equivalents of TEACl (red).

Table 4. Summary of Electrochemical Potential Data for Compounds 3 versus SCE[a]

compound	$E_{1/2}^{ox1}$ (V)	ΔE_p (mV)[b]	$E_{1/2}^{ox2}$ (V)	ΔE_p (mV)[b]
3a	0.92	125		
o-**3b**	0.48			
o-**3c**	1.15	120		
o-**3d**	0.90	80		
p-**3b**	1.05	70	1.33	82
p-**3c**	0.61	68	0.89	78
p-**3d**	0.81	65	1.10	68

[a]Electrochemical potentials in V vs SCE in CH_2Cl_2/0.2 M Bu_4NPF_6. Scan rate 50 mV s^{-1}. [b]Difference between peak potentials in mV.

different *o*-phenyl substituted triazenide ligands, $Pd_2[R{-}N{-}N{-}N{-}R']_2$ (R = R′ = *o*-$MeOC_6H_4$, *o*-$MeCO_2C_6H_4$, or *o*-ClC_6H_4; R = *o*-$MeCO_2C_6H_4$ and R′ = C_6H_5, *p*-BrC_6H_4 or *p*-MeC_6H_4). In compound *o*-**4b**, each triazenide ligand bridges the two metal centers and the palladium(I) is surrounded by one Pd, two N, and the Br from one of the two *ortho* pendent

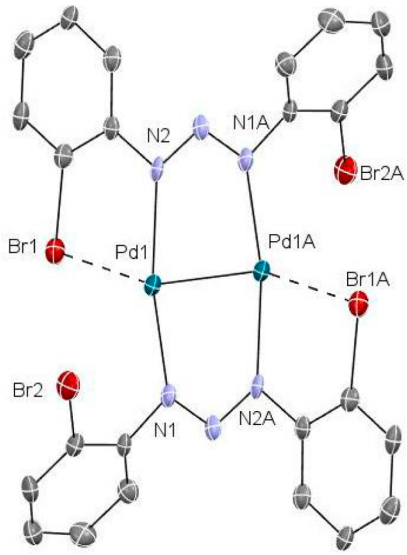

Figure 6. ORTEP view for compound *o*-**4b** with the H atoms omitted for clarity. Important bond distances (Å) and angles (deg) are Pd(1)–Pd(2), 2.5235(14); Pd(1)–N(1), 2.478(8); Pd(1)–N(2), 2.559(8); Pd(1)–Br(1), 2.7627(13); N(1)–Pd(1)–Pd(2), 88.97(16); N(1)–Pd(1)–N(2), 169.4(2).

Lewis basic group of the phenyltriazenide ligand, showing a distorted square planar geometry with N(1)–Pd(1)–N(2), N(1)–Pd(1)–Br(1), and N(1)–Pd(1)–Pd(1A) angles of 169.4(2), 112.74 (1), and 88.97(16)°, respectively. The complex has essentially planar bicyclic cores, formed by the two N_3-ligands and the $\{M_2\}$ unit.

The Pd(1)–Pd(2) distance of 2.5235 Å is consistent with a Pd–Pd bond, and it is longer than that observed for other dinuclear triazenide palladium(I) compounds (2.4148–2.4309 Å).[4b,d] The Pd(I)···Br and Pd(I)···OMe interactions have been studied by DFT calculations.

The structure of *o*-**4b** is similar to those side-by-side palladium(I) compounds of the type $Pd_2X_2(PP)_2$ (PP = bis(diphenylphosphino)methane, X= Cl, Br, C_6Cl_5, CF_3CO_2;[17a] PP = (*R*,*R*)-bis(*tert*-butylmethylphosphino)-methane, X = Br;[17b] PP = aminobis(*o*-methoxyphenylphosphonite), X = Br[17c]) with anionic ligands in axial positions, and

dx.doi.org/10.1021/om500702j | *Organometallics* 2014, 33, 5378–5391

the cationic $[Pd_2(PP)(CN^tBu)_2](BF_4)_2$ (PP = bis-(diphenylphosphino)methane.[17d] These compounds have no planar bicyclic cores, the dihedral angle (Φ) between the two planes formed by the two metal centers, and two phosphorus atoms from the ligands (PMMP) has values from 33.0 to 50.5°. The Pd−Pd distances are longer with values between 2.594 and 2.699 Å.[17a,c]

In a previous paper[18] we have published the synthesis and structural characterization of the compound $Pd_2[\mu\text{-}C_9H_8NPPh_2]_2(NCCH_3)_2$ in which the two palladium(I) metal centers are bridged by two P,N-ligands obtained by deprotonation of the indolyl nitrogen in the diphenyl(3-methyl-2-indolyl) phosphine, $C_9H_8NPPh_2$. Two acetonitrile molecules are coordinated in axial positions. The Pd−Pd distance is 2.5459(8) Å, and, in this case, the Φ value (37.05°) is bigger due to higher steric and orbital interactions minimized by a higher twisting about the Pd−Pd axis.

C. Dinuclear Palladium(III) Compounds with Bridging Triazenide Ligands. The reversibility observed for the Pd_2^{5+}/Pd_2^{4+} and Pd_2^{6+}/Pd_2^{5+} processes in most of the compounds of type **3** suggested that they are suitable starting materials to access the high-valent dinuclear palladium compounds. Further evidence of their suitability could be obtained by adding chloride in the axial positions when the electrochemical oxidation was performed in the presence of TEACl. Additionally, previous DFT calculations verified that the formation of Pd−Cl bonds can stabilize some dinuclear palladium(III) compounds.[8c,d] These observations prompted us to undertake the synthesis of new palladium(III) compounds by chemical oxidation with $PhICl_2$.

Chemical Oxidation of Compounds ***3***. In an attempt to synthesize new palladium(III) compounds of general formula $Pd_2[(C_6H_4)PPh_2]_2[R{-}N{-}N{-}N{-}R]_2Cl_2$ we have monitored by ^{31}P NMR spectroscopy from 200 to 298 K the reaction of compounds of type **3** with the oxidant $PhICl_2$ (Scheme 2). These experiments allowed us to get information about the stability of the palladium(III) compounds obtained.

Scheme 2. Reaction of 3 with $PhICl_2$ To Give Dinuclear Palladium(III) Compounds, $Pd_2[(C_6H_4)PPh_2]_2[R{-}N{-}N{-}N{-}R]_2Cl_2$ (5)

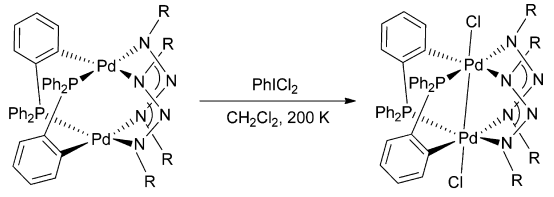

3; *o*-**3b-d**; *p*-**3b-d** **5**; *o*-**5c,d**; *p*-**5b-d**

R = C_6H_5 (**a**); BrC_6H_4 (**b**); $MeOC_6H_4$ (**c**); *o*-MeC_6H_4 (**d**)

$PhICl_2$ was added at 200 K to a solution of the corresponding dinuclear palladium(II) compound (stoichiometric ratio $PhICl_2/Pd_2$: 1/1) in CD_2Cl_2 in a NMR tube, and immediately the ^{31}P NMR spectrum was recorded and the date was listed in Table 1. In agreement with the literature, the appearance of one signal shifted toward high fields around 30 ppm in relation to that observed for the corresponding compound **3** indicates the formation of a palladium(III) compound.[8] Compounds **5a**, *p*-**5b**, *p*-**5c**, and *p*-**5d** with bridging non-*o*-phenyl substituted triazenide ligands were obtained as the only product of the reaction, their ^{31}P NMR spectra showed a single signal around −35 ppm. No *o*-**5b** was obtained because of the fairly strong Pd···Br interaction that blocks the axial sites preventing the reaction with chlorine. The less strong Pd···OMe interaction allows the oxidation of *o*-**3c** giving a mixture of compounds as shown by the ^{31}P NMR spectrum. Some steric considerations also need to be taken into account, compound *o*-**3d** with *o*-Me groups gave also a mixture of oxidized compounds, and the ^{31}P NMR spectrum showed signals at higher fields suggesting that the product was oxidized but no Pd−Cl bonds were formed.

Compounds **5a** and *p*-**5b** were relatively stable at room temperature, and they have been synthesized and characterized by ^{13}C, ^1H, and ^{31}P NMR spectroscopy at 223 K. Unfortunately suitable crystals for X-ray diffraction methods could not be obtained.

D. DFT Studies of Pd(I), -(II), and -(III) Compounds. *Stability of the Palladium(I) Compounds.* The preparation of these palladium(I) compounds is associated with the characteristics of the *o*-phenyl substituents in the triazenide ligands that interact in the axial positions. Walsh and co-workers compared the behavior of some *o*-substituted phenyltriazenides, while only palladium(I) compounds were obtained with $MeCO_2$ and MeO substituted triazenides, the one with a MeS group gave a palladium(II) compound. The authors consider that the greater donating ability of the MeS group results in a more electron rich palladium center, more stable to the reduction.[4b]

We have studied computationally the relative stability of the Pd(I) compounds by calculating the substituent effect on the relative energies of a model reaction $Pd_2L_2 + 2L'H \Rightarrow Pd_2L'_2 + 2LH$, where L represents the nonsubstituted triazenide ligand and L′ represents the ligands substituted with Br, OMe, and Me substituents. Table 5 lists the reaction energies for the *ortho*- and *para*-substituted complexes relative to the nonsubstituted one.

Table 5. Effect of the Substitution of the Triazenide Ligands on the Reaction Energies of the Model Reaction $Pd_2L_2 + 2L'H \Rightarrow Pd_2L'_2 + 2LH$

	ΔE_r [kJ mol^{-1}][a]	
Pd(I) compound	*ortho*	*para*
4a	0	
4b	−231	+1
4c	−29	−5
4d	+33	−2

[a]Relative to the energy of nonsubstituted structure **4a**.

The results show a clear preference of the *o*-Br phenyl substituted ligand to form a stable Pd(I) complex. The enhanced stability has to be due to structural interactions, since the *para*-substituted ligands are notably less favorable than *o*-**4b**. Also *o*-**4c** is somewhat stabilized compared to **4a**. Figure 7 presents the optimized structures *o*-**4b** and *o*-**4c** which have additional intramolecular interactions at the axial sites of the complexes. The most important properties of the electronic density at the bond critical points corresponding to these intramolecular interactions are shown in Figure 7.

Figure 7 verifies the importance of the axial interactions on the stability of the Pd(I) complexes and explains why the *o*-Br and *o*-MeO phenyl substituted ligands are the preferred ones in forming the reduced Pd(I) complex. Although the axial interactions were mostly noncovalent in nature, as can be

dx.doi.org/10.1021/om500702j | *Organometallics* 2014, 33, 5378−5391

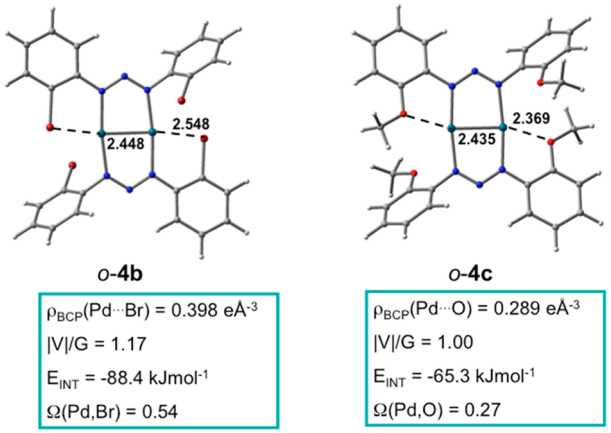

Figure 7. Optimized structures of the Pd(I) complexes *o*-**4b** and *o*-**4c** with selected intramolecular interactions. The properties of the electron density according to the QTAIM analysis are shown in the corresponding boxes for the axial Pd···Br and Pd···O interactions. ρ_{BCP} (Pd−X) = electron density at the bond critical point; $|V|/G$ = ratio between potential energy density and kinetic energy density; E_{INT} = interaction energy at the BCP, Ω(Pd,X) = delocalization index between atoms Pd and X.

seen in the value of $|V|/G$, which for pure electrostatic interactions gets the value of <1, the strength of the interaction was very large (E_{INT} was −88.4 kJ mol^{-1} and −65.3 kJ mol^{-1} for the Pd···Br and Pd···O interactions, respectively). For the delocalization index, which can be regarded as the bond index, we obtained values of 0.54 and 0.27, which are rather typical for noncovalent metal−ligand bonding. In both complexes *o*-**4b** and *o*-**4c**, the Pd−Pd bond index was about 1, showing strong metal−metal bonding with interaction energies of −104.5 kJ mol^{-1} and −106.8 kJ mol^{-1} at the bond critical points, respectively. The strong bonding between the Pd atoms was also seen in short Pd−Pd distances (Figure 7).

Structures of the Pd(II) and Pd(III) Triazenide Compounds. We performed geometry optimization of the different substitution options, which have been experimentally obtained, to gain insight on the favorability of the oxidation reactions.

All complexes were fully optimized at the DFT level of theory, and the geometries and electronic properties were compared with the previously studied palladium compounds with the formamidinate ligand.[8c] The effect of the different *ortho*- or *para*-phenyl substituents on the Pd−Pd distance in Pd(II) and Pd(III) compounds can be seen in Table 6.

Generally, the substituent effect was rather small, and results were very similar for the Pd−Pd distances in all triazenide ligands, which were substituted at the *para*-position of the phenyl groups. On the other hand, the *ortho*-substituted complexes *o*-**3b** and *o*-**3c** showed a rather different behavior of the energetically most favorable optimized structures (Figure S8). As already seen in the Pd(I) complexes, both *o*-Br and *o*-OMe phenyl substituents could interact with the palladium atoms at the axial site. The axial Pd···Br interactions resembled similar intramolecular interactions found already in the Pd(I) compound *o*-**4b**, but the interaction energy was rather much weaker in the case of Pd(II) than in the Pd(I) complex (E_{INT} was −41.4 kJ mol^{-1}, −26.4 kJ mol^{-1}, and −88.4 kJ mol^{-1} in *o*-**3b**, *o*-**3c**, and *o*-**4b**, respectively).

The energetically most favorable Pd(II) isomer was in most cases the *para*-substituted derivative, except with the *ortho*-substituted bromine, where the intramolecular Pd···Br interactions stabilized the structure. Because of this stabilization, the reaction of compound *o*-**3b** with an excess of triazenide ligand evolved more slowly toward the dinuclear palladium(I) compound, *o*-**4b**, than compound *o*-**3c** even though DFT calculations exhibited greater stability for compound **o-4b** than for *o*-**4c**.

The geometries of nearly all of the complexes agreed well with the obtained experimental crystal structures. However, there was one striking difference in the computational and experimental structures: compound *o*-**3b** with an *o*-Br substituted phenyl triazenide ligand showed a notably longer Pd−Pd distance and a shorter Pd···Br distance than was measured from the X-ray structure, 2.750 Å versus 2.713 Å and 2.856 Å versus 3.012 Å, respectively. A clear explanation for this difference can be obtained by inspecting the crystal structure in detail. The solid state structure consists of dinuclear molecules, which attach together with intermolecular Br···Br interactions, thus forming a chain of molecules (Figure S9).

The intermolecular interactions were studied further with a model of two adjacent molecules cut from the crystal structure. The QTAIM analysis showed that the intermolecular Br···Br interactions are weak and purely noncovalent (Table S1, compound *o*-**3b**_dim). However, they have an important effect on the solid state structure of the compound and also on the intramolecular interactions, such as the Pd···Pd distance.

Details of the interactions and the QTAIM analysis can be found in the Supporting Information (Tables S1−S3). Since the weak intermolecular interactions are not normally present in solution, the computational results of single molecules will give reliable information on the relative electronic effects of different ligands.

According to the QTAIM analysis, the Pd(II)···Pd(II) interaction in compounds type **3** shows some electron sharing,

Table 6. Effect of the Substitution of the Phenyl Triazenide Ligands on the Pd−Pd Distances in Palladium(II) and Palladium(III) Compounds

	Pd−Pd distances (Å)[a]				
	palladium(II) compounds			palladium(III) compounds	
compound	*ortho*	*para*	compound	*ortho*	*para*
3a	2.692 (2.6771)		**5a**	2.556	
3b	2.750 (2.7129)	2.691(2.6623)	**5b**	2.603	2.557
3c	2.705	2.693 (2.6794)	**5c**	2.592	2.559
3d	2.706 (2.6696)	2.692 (2.6618)	**5d**	2.595	2.557
[b]	2.736 (2.715)[d]	*c*	2.593[d]		

[a]Experimental distances in brackets. [b][$Pd_2[(C_6H_4)PPh_2]_2[C_6H_5N-C(H)-NC_6H_5]_2$; [c]$Pd_2[(C_6H_4)PPh_2]_2[C_6H_5-N-C(H)-N-C_6H_5]_2Cl_2$; [d]Reference 8c.

dx.doi.org/10.1021/om500702j | *Organometallics* 2014, 33, 5378−5391

and therefore the interaction is not entirely noncovalent, which is seen in the value ratio of the potential energy density and the kinetic energy density, $|V|/G > 1$. Also the negative and rather large interaction energy, ranging from −60 kJ mol^{-1} to −68 kJ mol^{-1}, indicate substantial interaction between the two palladium atoms. The bond delocalization index at the corresponding Pd−Pd bond critical point, which can be regarded as bond index, gets nonzero values around 0.35. The substituent effect of the triazenide ligands on the Pd−Pd bond is small, showing a slight preference for energies of the compounds with parasubstituted triazenide ligands. This strengthening of the Pd(II)···Pd(II) interaction is in line with the decreased metal−metal distance in the parasubstituted compounds.

As already noticed in the previous study of the O,O′-chelating ligands,[8d] the metal−metal bond shortens when the compound is oxidized from Pd_2^{4+} to Pd_2^{6+}. With the triazenide ligands the shortening was somewhat smaller than with the chelating ligands but rather similar than with the bridging carboxylates, about 0.15 Å.[8c,d] Similar contraction of the Pd−Pd bond distance in the oxidized Pd(III)−Pd(III) complexes was also found in the study of Powers and Ritter.[10] QTAIM analysis shows increased electron density and hence increased degree of covalency and bond delocalization index at the Pd(III)−Pd(III) BCPs. There is also a small but systematic increase in the corresponding interaction energies (Table S3).

When the Pd−Pd distance was compared with the previously studied Pd(II) and Pd(III) compounds with the formamidinate ligand, the difference in the electronic nature of the ligands could be seen in the computationally optimized Pd−Pd distances. It should be noted that the effect of ligand substitution was studied also in the case of the formamidinates.[8c] The Pd−Pd distances were shorter in the case of triazenides than in formamidinate, which results in slight differences in the properties of the charge density (Tables S2 and S3). However, in both triazenides and amidinates the trends were the same; the preferred Pd(II) isomer was the *ortho*-phenyl substituted one only for bromine substituent, since similar stabilizing axial Pd···Br interactions were possible.

Stability of the Oxidized Compounds. The stability of the oxidized compounds was studied by calculating the relative energies of the chemical oxidation model reaction:

$$Pd_2[(C_6H_4)PPh_2]_2[R{-}N{-}N{-}N{-}R]_2 + Cl_2 \Rightarrow Pd_2[(C_6H_4)PPh_2]_2[R{-}N{-}N{-}N{-}R]_2Cl_2$$

Table 7 lists the obtained reaction energies. Again, the various triazenide compounds are compared with the corresponding formamidinate compounds.

As can be expected, the compounds with *para*-substituted phenyl groups in the triazenide ligands were more readily oxidized with axial chloride ions than the *ortho*-substituted ones. Furthermore, when the phenyl groups had a Br substituent at the *ortho*-position, the fairly strong interaction with the Pd atoms blocked the axial site inhibiting the reaction with chloride. This is well in agreement with the experimental findings, since no palladium(III) compound was obtained by reaction of *o*-**3b** with $PhICl_2$ at 200 K. With the *o*-OMe substituted ligand the Pd···O interaction was weak enough to be overcome with the stronger Pd−Cl bond; therefore, the oxidized compound was found feasible. The ^{31}P NMR spectrum of the reaction of *o*-**3c** with $PhICl_2$ at 200 K showed two signals at shift values corresponding to palladium(III) compounds. Otherwise, the reaction energies were very similar to the corresponding formamidinate ligands, suggesting similar behavior upon oxidation.

Table 7. Effect of the Substitution of the Phenyl Triazenide Ligands on the Reaction Energies of the Oxidation Model Reaction

	ΔE_r [kJ mol^{-1}]	
oxidation reaction with Cl_2	*ortho*	*para*
3a → **5a**	−88	
3b → **5b**	+96	−91
3c → **5c**	−87	−96
3d → **5d**	−75	−92
a	−84	

[a] $Pd_2[(C_6H_4)PPh_2]_2[C_6H_5N{-}C(H)\text{-}NC_6H_5]_2 \rightarrow Pd_2[(C_6H_4)\text{-}PPh_2]_2[C_6H_5{-}N{-}C(H){-}N{-}C_6H_5]_2Cl_2$.

E. Metalated Palladium(II) and -(III) Compounds As Precatalysts in the Direct Phenylation of Indole. Compounds **3**, **5a**, and *p*-**5b** have been tested as precatalysts in the direct 2-phenylation of the *N*-unprotected indole (**6**) at room temperature with $[Ph_2I]PF_6$ in acetic acid to give compound **7** (Scheme 3). The reaction has been followed by ^1H NMR spectroscopy. The results are displayed in Table 8.

With compound **3a** and under the conditions described in Scheme 3, the 2-phenylation of indole proceeded in only 7 h giving an isolated yield for **7** of 88% (Table 8, entry 1). In the same reaction conditions, *o*-**3c** and *p*-**3b**−**d** gave high yields (81−84%) but with higher reactions times (19−96 h) (Table 8, entries 3−6). Compounds *o*-**3b** and *p*-**3b**−**d** showed some insolubility in acetic acid nevertheless they showed activity (Table 8 entries 2, 4−6). With the insoluble compounds the reaction was also performed with addition of CH_2Cl_2 until their complete solution and different results were obtained. With the most insoluble compound *o*-**3d** the reaction was completed in 24 h giving the highest isolated yield (99%) observed (Table 8, entry 10). On the other hand, when *p*-**3b** was used, the reaction was complete in half time (96 → 48 h) increasing the yield for **7** up to 87% (Table 8 entry 11), but in the case of *o*-**3b** the time was significantly reduced (264 → 48 h) although the yield decreased from 78 to 64% (Table 8, entry 9). With *p*-**3c**,**d** the reaction was complete in the same reaction time, but in both cases a significant decrease was observed in the isolated yield for **7** (Table 8, entries 12 and 13).

Results published by Sanford and co-workers showed a yield of 81% and a longer reaction time (15 h) for this reaction using $[Ph_2I]BF_4$ as oxidant and $IMeSPd(OAc)_2$ (IMes = 1,3-bis(2,4,6-trimethylphenyl)-imidazol-2-ylidene) as potential catalyst.[15]

The isolated palladium(III) compounds have also been tested in the catalytic reaction. Compounds **5a** gave **7** in a shorter time and a higher yield than *p*-**5b** (24 versus 48 h and 76 versus 59%, respectively) (Table 8, entries 7 and 8).

When the reaction was developed without the presence on palladium complexes, compound **7** was not observed.

At the end of each reaction a reddish solid was obtained. The electron microscopy spectrum of the isolated solid showed that it contains mostly fluorine with some palladium. The isolated reddish solid did not catalyze the phenylation reaction. The HPF_6 obtained by reaction of $[Ph_2I]PF_6$ with acetic acid decomposed at room temperature giving HF, which attacks the glass Schlenk tubes.[19]

dx.doi.org/10.1021/om500702j | *Organometallics* 2014, 33, 5378−5391

Scheme 3. Direct Phenylation of Indole

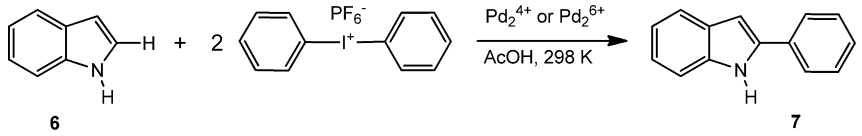

Table 8. 2-Phenylation of Indole with Compounds Type 3, 5a, and *p*-5b as Precatalyst

entry	conditions	precatalyst	reaction time (h)	7 yield (%)
1	Scheme 3	**3a**	7	88
2		*o*-**3b**	264	78
3		*o*-**3c**	48	84
4		*p*-**3b**	96	84
5		*p*-**3c**	20	81
6		*p*-**3d**	19	82
7		**5a**	24	76
8		*p*-**5b**	48	59
9	Scheme 3 + addition of CH_2Cl_2	*o*-**3b**	48	64
10		*o*-**3d**	24	99
11		*p*-**3b**	48	87
12		*p*-**3c**	19	68
13		*p*-**3d**	19	66

Since the carboxylate and formamidinate ligands are isoelectronic with the triazenide ones, we have tested some of the these orthometalated formamidinate and carboxylate dinuclear palladium(II) compounds in this catalytic reaction. The results listed in Table 9 were compared with the previous obtained with the triazenide derivatives (Table 8).

With the carboxylate derivatives, $Pd_2[(C_6H_4)PPh_2]_2[O_2CCH_3]_2$ and $Pd_2[(C_6H_4)PPh_2]_2[O_2CCF_3]_2$, **7** was obtained in higher yields and reaction times in intermediate values in relation to those observed for the triazenide derivatives (Table 9, entries 1 and 2).

In the case of the formamidinate derivatives, $Pd_2[(C_6H_4)PPh_2]_2[(C_6H_4)NC(H)N(C_6H_4)]_2$, $Pd_2[(C_6H_4)PPh_2]_2[(p\text{-}CH_3C_6H_4)NC(H)N(p\text{-}CH_3C_6H_4)]_2$, and $Pd_2[(C_6H_4)PPh_2]_2[(p\text{-}CH_3OC_6H_4)NC(H)N(p\text{-}CH_3OC_6H_4)]_2$, the yields were lower with low reaction time for the two first products (Table 9, entries 3−5).

In a previous paper we have tested the dinuclear palladium(II) compounds with [O−O] donor ligands, $Pd_2[(C_6H_4)PPh_2]_2[acac]_2$ and $Pd_2[(C_6H_4)PPh_2]_2[C_6H_4OC(O)CH_3]_2$, in the similar catalytic reaction of room temperature direct 2-phenylation of 1-methylindole, showing to be excellent precatalysts giving high isolated yields in 2-phenyl-1-methylindole with short reaction times (93 and 91% and 2 and 6 h, respectively).[8d] Applied as a precatalyst in the catalytic reaction studied in this paper, low yields for **7**, 37 and 59% and reaction times of 15 and 20 h were respectively obtained (Table 9, entries 6 and 7).

Lower yields for **7** and longer reaction times were obtained (Table 9, entries 10 and 11) when the orthometalated mononuclear palladium(II) compounds $Pd[(C_6H_4)PPh_2]BrPPh_3$ and $Pd_2[(C_6H_4)PPh_2]_2[C_6H_4OC(O)CH_3]_2$, in which redox cooperation is not possible, were used as precatalysts.

Investigation on the 2-Phenylation of Indole. Sanford and co-workers with mononuclear palladium(II) compounds proposed that this reaction proceeds via a mononuclear Pd(IV)-phenyl intermediate.[13,15c] On the other hand, also dinuclear palladium(III) complexes have been proposed as active species for several catalytic reactions.[14] Especially, Sanford, Yates, and co-workers have suggested that a phenylated dinuclear palladium(III) cation would initiate the catalysis cycle in the formation of mppPh (mpp = 3-methyl-2-phenylpyridine).[20]

In the search for the possible first step in the catalytic oxidation process in the 2-phenylation of indole with dinuclear palladium(II) compounds and whereas its oxidation enables the access to dinuclear palladium(III) compounds, we have explored the Pd(III) intermediate by performing DFT calculations on the axial Pd-Ph interactions.

We optimized the compounds with axial phenyl ligands and compared the relative stability of the products by calculating the stabilization energies as well as the effect of the interaction to the nature of the Pd−Pd bonds. Table 10 shows the relative stability energies (referenced to the most favorable reaction energy in *p*-**3c**) and the Pd−Pd and Pd−C(Ph) bond distances for the bisphenyl derivatives.

Interaction of two phenyls with the palladium atoms at the axial sites was sterically very demanding because of the bulky phenyl groups in both the metalated phosphines and the

Table 9. 2-Phenylation of Indole with Dinuclear and Mononuclear Palladium(II) and -(III) Compounds

	entry	conditions	precatalyst	reaction time (h)	7 yield (%)
	1	Scheme 3	$Pd_2[(C_6H_4)PPh_2]_2[O_2CCH_3]_2$	21	98
dinuclear compounds	2		$Pd_2[(C_6H_4)PPh_2]_2[O_2CCF_3]_2$	36	98
	3		$Pd_2[(C_6H_4)PPh_2]_2[(C_6H_4)N-C(H)-N(C_6H_4)]_2$	13	79
	4		$Pd_2[(C_6H_4)PPh_2]_2[(o\text{-}MeC_6H_4)N-C(H)-N(4\text{-}CH_3C_6H_4)]_2$	11	71
	5		$Pd_2[(C_6H_4)PPh_2]_2[(o\text{-}MeOC_6H_4)N-C(H)-N(4\text{-}CH_3OC_6H_4)]_2$	120	66
	6		$Pd_2[(C_6H_4)PPh_2]_2[acac]_2$	15	37
	7		$Pd_2[(C_6H_4)PPh_2]_2[C_6H_4OC(O)CH_3]_2$	20	59
	8	Scheme 3 + addition of CH_2Cl_2	$Pd_2[(C_6H_4)PPh_2]_2[O_2CCH_3]_2Cl_2$	168	44
	9		$Pd_2[(C_6H_4)PPh_2]_2[O_2CCF_3]_2Cl_2$	168	59
mononuclear compounds	10		$Pd[(C_6H_4)PPh_2]BrPPh_3$	168	86
	11		$Pd[(C_6H_4)PPh_2]Br[(4\text{-}BrC_6H_4)PPh_2]$	168	96

dx.doi.org/10.1021/om500702j | *Organometallics* 2014, 33, 5378−5391

Table 10. Effect Axial Interaction of Phenyl Groups on the Relative Stability of the Compounds 3a, *o*-3b−d, and *p*-3b−d and the Corresponding Pd−Pd and Pd−C(Ph) Distances

		ΔE [kJ mol^{-1}]		Pd−Pd [Å]		Pd−C(Ph) [Å]	
compound	substituent	*ortho*	*para*	*ortho*	*para*	*ortho*	*para*
3a	H	17		2.745		2.186	
3b	Br	195	40	2.816	2.712	2.170	2.208
3c	OMe	23	0	2.775	2.790	2.180	2.147
3d	Me	36	15	2.807	2.746	2.173	2.183
[a]	H	11		2.840		2.168	

[a] $Pd_2[(C_6H_4)PPh_2]_2[C_6H_5N{-}C(H){-}NC_6H_5]_2$.

triazenide ligands. However, we were able to find optimized structures for all compounds, even if the relative stability of the products with *ortho*-substituted ligands was poor at least in the case of the *o*-Br triazenide compound. The weaker stability of the *ortho*-bromide substituted compounds was not entirely due to steric effects, since also the para-substituted derivative showed somewhat poorer stability. The substituent effect on the stability trends was also consistent with the experimental reaction times in the catalytic phenylation of indole, since the Br-substituted catalysts *o*-**3b** and *p*-**3b** led to longer reaction times, thus indicating less stability of the intermediate compound.

The stability of the complexes could be mostly related to the differences in the Pd−C(Ph) distances in the products, the shorter the distance, the better the stability. Furthermore, shorter Pd−C(Ph) distances led to longer Pd−Pd distances, as can be seen in Table S4, contrary to the interaction with axial chlorides, where stronger Pd−Cl interaction shortened the Pd−Pd distance and led to formation of the Pd−Pd bond with considerable covalent character. Figure 8 shows the properties of the electron density at the corresponding bond critical points for the nonsubstituted complexes **3a** and **5a** and the corresponding intermediate **3a+2Ph**. The large electron density

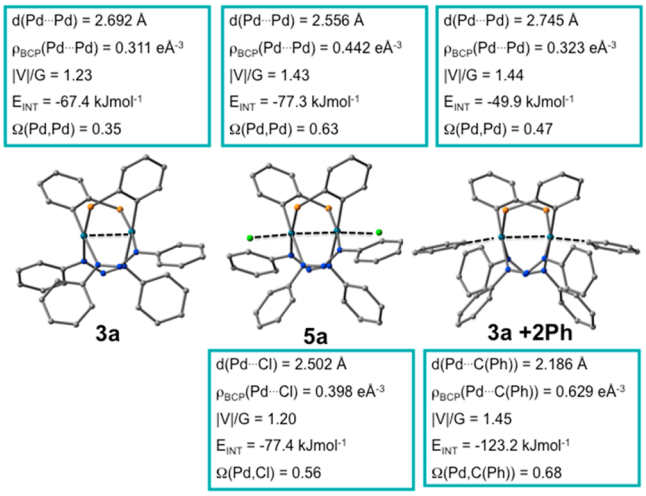

Figure 8. Comparison of the properties of the Pd−Pd and the axial interactions in complexes type **3a**, **5a**, and **3a+2Ph**. Hydrogens and free phenyl groups of the phosphines have been omitted for clarity. The properties of the electron density according to the QTAIM analysis are shown in the corresponding boxes for the PdPd and Pd···C(Ph) interactions. ρ_{BCP} (Pd−X) = electron density at the bond critical point; $|V|/G$ = ratio between potential energy density and kinetic energy density; E_{INT} = interaction energy at the BCP, Ω(Pd,X) = delocalization index between atoms Pd and X.

at the BCP and the large interaction energy supported the strong nature of the Pd−C(Ph) bond.

As we have observed earlier,[8e] interaction with axial chlorides changes the nature of the Pd···Pd interaction by reducing the bond distance and increasing the covalent nature of the interaction, as can be seen in the increased $|V|/G$ ratio from 1.23 to 1.43 for **3a** and **5a**, respectively. The axial interaction also slightly increased the strength of the Pd···Pd interaction. Also axial interaction with phenyl groups in the intermediate structure had the same effect of increasing the covalent nature of the bond between the palladium atoms, even though the distance between palladiums was larger and the strength of the interaction smaller than in **3a** (Figure 8). However, when the properties of the axial Pd···Cl and Pd···C(Ph) interactions were compared, the interaction with the axial phenyls proved to be very strong (E_{INT} = −123.2 kJ mol^{-1}), approaching the strength of covalent bonding, which is most probably due to larger electron density at the Pd···C(Ph) bond critical point. The strong Pd···C(Ph) bonding is the source of enhanced stability of the intermediate structures and supports also the experimental suggestion that the axial Pd−Cl interaction can be replaced with the axial Pd−Ph interaction. We also optimized a monophenylated Pd(III) complex with one axial phenyl group and one chloride ligand and performed a QTAIM analysis for the nature of the interactions. According to the results shown in Figure S10, there is a strong axial effect from the phenyl group which reduces the strength of the opposite Pd−Cl interaction and facilitates the removal of the second chlorine and formation of the bisphenylated complex.

Therefore, the bisphenylated intermediate is a very feasible option for the catalytic 2-phenylation of indole. Furthermore, similar intermediate structures can be effective in the phenylation process involving both bimetallic Pd(II) and Pd(III) complexes.

CONCLUSION

In a nutshell, the *ortho*- and *para*-phenyl substituted triazenides have shown to be very suitable ligands in the synthesis of new dinuclear palladium compounds in a wide range of oxidation states: I, II, and III. Compounds of the general formula $Pd_2[(C_6H_4)PPh_2]_2[R{-}N{-}N{-}N{-}R]_2$ can undergo a reduction or oxidation process giving respectively $Pd_2[R{-}N{-}N{-}N{-}R]_2$ or $Pd_2[(C_6H_4)PPh_2]_2[R{-}N{-}N{-}N{-}R]_2Cl_2$ compounds. All the compounds have been characterized by NMR spectroscopy and some of them also by X-ray diffraction methods. DFT calculations verified the importance of the mostly noncovalent Pd···Br or Pd···OMe axial interactions on the stability of the palladium(I) compounds, $Pd_2[R{-}N{-}N{-}N{-}R]_2$, versus the corresponding ones in oxidation state II, $Pd_2[(C_6H_4)$-$PPh_2]_2[R{-}N{-}N{-}N{-}R]_2$. Under cyclic voltammetric conditions, the triazenide dinuclear palladium(II) compounds type **3**

dx.doi.org/10.1021/om500702j | *Organometallics* 2014, 33, 5378−5391

were oxidized showing one (**3a**, *o*-**3c**-**d**) or two reversible (*p*-**3b**−**d**) waves assigned to Pd_2^{5+}/Pd_2^{4+} and Pd_2^{6+}/Pd_2^{5+} couples. When the electrochemical oxidation was carried out in the presence of chloride, the loss of two electrons is followed by the addition of two chlorides giving the Cl−Pd(III)−Pd(III)−Cl species that have been detected, showing the accessibility of the palladium(II) compounds to ones in a high-valent oxidation state, III. The chemical oxidation of compounds **3** with $PhICl_2$ allowed to isolate two new unusual dinuclear palladium(III) compounds, $Pd_2[(C_6H_4)PPh_2]_2[R{-}N{-}N{-}N{-}R]_2Cl_2$ (R = C_6H_5, **5a**; R = *p*-BrC_6H_4, *p*-**5b**), that were characterized by spectroscopic techniques at low temperatures.

The computational studies showed that the energetically most favorable palladium(II) complexes were the ones with *para*-substituted phenyltriazenide, except in the case of the *ortho*-substituted bromine derivative where the intramolecular Pd···Br interaction stabilized its structure. Also the DFT calculations are in agreement with the experimental finding that we did not succeed in obtaining the *o*-Br phenyltriazenide palladium(III) derivative, because the fairly strong Pd···Br interaction can block the axial site inhibiting the addition of chloride.

The isolated palladium(II) and (III) compounds were tested in the direct phenylation of indole at room temperature with $[Ph_2I]PF_6$ in acetic acid. In the case of **3a** the reaction proceeded with the lowest reaction time, 7 h, and with an 88% isolated yield, better results than that published by Sanford and co-workers, 15 h, and 81% with a mononuclear palladium(II) compound as precatalyst. The highest yield, 99%, was obtained with *o*-**3d** and addition of CH_2Cl_2 to the reaction medium but with a higher reaction time, 24 h. DFT calculations have been executed in order to study the possible first step in this catalytic reaction. The formation of the Pd(III) intermediate compounds have been explored considering the axial Pd−(C)Ph interactions that have been proved to be stronger than the Pd−Cl ones (E_{INT} = −123.2 kJ mol^{-1} versus E_{INT} = −77.4 kJ mol^{-1}).

EXPERIMENTAL SECTION

All the reactions were carried out under a dry nitrogen atmosphere using Schlenk techniques. Solvents were purified according to standard procedures. Commercially available reagents were used as purchased. $[Pd((C_6H_4)PPh_2)Br]_4$,[21] **1**, and iodobenzene dichloride ($PhICl_2$)[22] were synthesized according to literature procedures. The triazenes were prepared by the procedure adapted from the literature involving the diazotation and coupling of anilines.[23] Solvent mixtures are v/v mixtures. Column chromatography was performed on silica gel (35−70 mesh).

NMR spectra were recorded on Bruker 400 and 500 AMX spectrometers as solutions in deuterated chloroform or dichloromethane at 298 K and low temperature. Chemical shifts are reported in ppm, using TMS (^{1}H, ^{13}C) and 85% H_3PO_4 (^{31}P) as references. The coupling constants (*J*) are in hertz (Hz).

Elemental analysis was provided by SCSIE of University of Valencia.

X-ray structure determinations were carried out on a Bruker Nonius Kappa CCD diffractometer (Mo Kα radiation, λ = 0.71073 Å). The structures were solved by direct methods using SHELXTL software package.[24] The correct positions for the heavy atoms were deduced from an *E* map. Subsequent least-squares refinement and difference Fourier calculations revealed the positions of the remaining non-hydrogen atoms. Hydrogen atoms were placed in geometrically generated positions and refined riding on the atom to which they are attached.

The electrochemical studies were carried out at room temperature with a 273 A PAR potentiostat in a three-electrode cell. The working electrode was a Pt electrode with a surface of 3.1 mm^2, the counter electrode a Pt wire, and the reference electrode Ag/AgCl (saturated KCl). The solvent was CH_2Cl_2−0.2 M Bu_4NPF_6, the solution was 0.5 mM for compounds, and the scan rate was 50 mV/s. In these conditions E_a for the couple Fc/Fc^+ was 0.550 V.

Synthesis of the Silver Triazenide Salts, Ag[R−N−N−N−R]. The silver salts were prepared as follows. In a 1:1 stoichiometric ratio, a solution of $AgNO_3$ in water (1 mL) was added under vigorous stirring to a CH_2Cl_2 solution (2 mL) of the corresponding triazene (0.5 mmol) previously deprotonated with a methanolic solution of NaOMe. Yellow precipitates were obtained in all the cases. Each solid was filtered, washed with MeOH (2 × 4 mL), and vacuum-dried. They were used without further purification. Yields: 135.1 mg (87%) R = C_6H_5; 226 mg (98%) R = *o*-BrC_6H_4; 217 mg (94%) R = *p*-BrC_6H_4; 134 mg (81%) R = *p*-MeC_6H_4.

Preparation of $Pd_2[(C_6H_4)PPh_2]_2[R{-}N{-}N{-}N{-}R]_2$, R = C_6H_5 (3a), R = *o*-BrC_6H_4 (*o*-3b), R = *p*-BrC_6H_4 (*p*-3b), R = *p*-MeC_6H_4 (*p*-3d). Compounds were prepared by reaction of compound **1** with the corresponding silver triazenide. $[Pd((C_6H_4)PPh_2)Br]_4$ (**1**) (100 mg, 0.056 mmol) was suspended in CH_2Cl_2 (10 mL), and the corresponding silver triazenide (0.224 mmol) was added. The reaction mixture was allowed to stir for 24 h after which the crude was filtered through a short plug of Celite. The solution was evaporated to dryness, and the solid precipitated by the addition of hexane was collected by filtration and washed with hexane. Orange-yellow microcrystalline powders were obtained by this method. Yields: 59.6 mg (48%) **3a**; 143.6 mg (89%) *o*-**3b**; 129.3 mg (80%) *p*-**3b**; 101.6 mg (77%) *p*-**3d**.

Characterization Data for ***3a****.* ^{1}H NMR ($CDCl_3$, 500 MHz, 298 K) δ 7.69 (m, 4H, ar), 7.52 (m, 2H, ar), 7.41 (m, 4H, ar), 7.30 (m, 4H, ar), 7.21 (m, 8H, ar), 7.10 (m, 8H, ar), 6.91 (m, 8H, ar), 6.81 (m, 8H, ar), 6.57 (m, 2H, ar); ^{31}P NMR ($CDCl_3$, 202 MHz, 298 K) δ 3.3 (s); ^{13}C NMR ($CDCl_3$, 125 MHz, 298 K) δ 163.0 (m, C metalated), 151.4 (s, C−N, trans to C), 150.7 (t, C−N, trans to P, $^3J_{P-C}$ = 2 Hz), 141.4−121.4 (ar). Anal. Calcd for $C_{60}H_{48}N_6P_2Pd_2$: C, 63.38; H, 4.25; N 7.45. Found: C, 62.73; H, 3.82; N 7.02.

X-ray Crystal Structure Data for ***3a*** *(CCDC 996514).* Empirical formula: $C_{60}H_{48}N_6P_2Pd_2{\cdot}CH_2Cl_2$, crystal system: monoclinic, space group: *P*2(1)/*n*, *a* = 11.147 (2) Å, *b* = 25.517 (5) Å, *c* = 19.740 (4) Å, β = 103.50 (3)°, *V* = 5459.6 (19) $Å^3$, *Z* = 4 crystal dimensions: 0.25 × 0.25 × 0.23 mm^3; MoK_α radiation, 273 (2) K; 30002 reflections, 10975 independent; (μ = 0.861 mm^{-1}); refinement (on F^2) with SHELXTL (version 6.1), 659 parameters, 0 restraints, R_1= 0.0510 ($I > 2\sigma$) and wR_2 (all data) = 0.1507, GOF = 1.108, max/min residual electron density: 1.397/−1.102 e $Å^{-3}$.

*Characterization Data for o-****3b****.* ^{1}H NMR ($CDCl_3$, 500 MHz, 298 K) δ 7.42 (m, 2H, ar), 7.37 (m, 8H, ar), 7.25 (m, 2H, ar), 7.10 (m, 4H, ar), 7.02 (m, 4H, ar), 6.93 (m, 4H, ar), 6.84 (m, 10H, ar), 6.73 (m, 8H, ar), 6.39 (m, 2H, ar); ^{31}P NMR ($CDCl_3$, 202 MHz, 298 K) δ 0.7 (s); ^{13}C NMR ($CDCl_3$, 125 MHz, 298 K) δ 165.4 (m, C metalated), 151.5 (t, C−N, trans to P, $^3J_{P-C}$ = 2 Hz), 150.1 (s, C−N, trans to C), 142.5−113.0 (ar). Anal. Calcd for $C_{60}H_{44}$ $Br_4N_6P_2Pd_2$: C, 49.90; H, 3.05; N 5.82. Found: C, 49.44; H, 2.87; N 5.58.

*X-ray Crystal Structure Data for o-****3b*** *(CCDC 996515).* Empirical formula: $C_{60}H_{44}Br_4N_6P_2Pd_2$, crystal system: monoclinic, space group: *C*2/*c*, *a* = 17.970 (4) Å, *b* = 13.656 (3) Å, *c* = 22.774 (5) Å, β = 102.97 (3)°, *V* = 5.446.2 (19) $Å^3$, *Z* = 4, crystal dimensions: 0.26 × 0.24 × 0.22 mm^3; MoK_α radiation, 273 (2) K; 14924 reflections, 5536 independent; (μ = 3.700 mm^{-1}), refinement (on F^2) with SHELXTL (version 6.1), 334 parameters, 0 restraints, R_1= 0.0427 ($I > 2\sigma$) and wR_2 (all data) = 0.1370, GOF = 1.140, max/min residual electron density: 0.885/−1.516 e $Å^{-3}$.

*Characterization Data for p-****3b****.* ^{1}H NMR ($CDCl_3$, 500 MHz, 298 K) δ 7.37 (m, 4H, ar), 7.30 (m, 2H, ar), 7.21 (m, 2H, ar), 7.09 (m, 12H, ar), 6.99 (m, 4H, ar), 6.89 (m, 4H, ar), 6.81 (m, 4H, ar), 6.69 (m, 4H, ar), 6.63 (m, 4H, ar), 6.46 (m, 4H, ar); ^{31}P NMR ($CDCl_3$, 202 MHz, 298 K) δ 3.8 (s); ^{13}C NMR ($CDCl_3$, 125 MHz, 298 K) δ 161.6 (m, C metalated), 150.1 (s, C−N, trans to C), 149.3 (t, C−N, trans to P, $^3J_{P-C}$ = 2 Hz), 141.2−116.3 (ar). Anal. Calcd for $C_{60}H_{44}$ $Br_4N_6P_2Pd_2$: C, 49.90; H, 3.05; N 5.82. Found: C, 49.50; H, 3.25; N 5.42.

dx.doi.org/10.1021/om500702j | *Organometallics* 2014, 33, 5378−5391

*X-ray Crystal Structure Data for p-**3b** (CCDC 996518).* Empirical formula: $C_{60}H_{44}Br_4N_6P_2Pd_2$, crystal system: monoclinic, space group: $P2(1)/c$, a = 10.9730 (4) Å, b = 23.5120 (5) Å, c = 22.6210 (9) Å, β = 103.2150 (14)°, V = 5681.6 (3) Å^3, Z = 4, crystal dimensions: 0.27 × 0.25 × 0.21 mm^3, MoK$_\alpha$ radiation, 273 (2) K; 20424 reflections, 12699 independent, (μ = 1.687 mm^{-1}), refinement (on F^2) with SHELXTL (version 6.1), 667 parameters, 0 restraints, R_1= 0.0563 ($I > 2\sigma$) and wR_2 (all data) = 0.1767, GOF = 1.065, max/min residual electron density: 1.054/−1.037 e Å^{-3}.

*Characterization Data for p-**3d**.* ^{1}H NMR ($CDCl_3$, 500 MHz, 298 K) δ 7.43 (m, 4H, ar), 7.34 (m, 2H, ar), 7.16 (m, 2H, ar), 7.11 (m, 4H, ar), 7.07 (m, 2H, ar), 6.95 (m, 8H, ar), 6.77 (m, 12H, ar), 6.65 (m, 8H, ar), 6.44 (m, 2H, ar), 2.14 (s, 12H, CH_3); ^{31}P NMR ($CDCl_3$, 202 MHz, 298 K) δ 3.4 (s); ^{13}C NMR ($CDCl_3$, 125 MHz, 298 K) δ 163.4 (m, C metalated), 149.2 (s, C−N, trans to C), 148.4 (t, C−N, trans to P, $^3J_{P-C}$ = 2 Hz), 141.4−121.2 (ar), 20.8 (s, CH_3). Anal. Calcd for $C_{64}H_{56}N_6P_2Pd_2$: C, 64.93; H, 4.73; N 7.10. Found: C, 64.65; H, 4.98; N 6.60.

*X-ray Crystal Structure Data for p-**3d** (CCDC 996520).* Empirical formula: $C_{64}H_{56}N_6P_2Pd_2$, crystal system: monoclinic, space group: $P2(1)/c$, a = 10.9050 (3) Å, b = 23.3620 (6) Å, c = 22.4590 (6) Å, β = 102.3250 (14)°, V = 5589.8 (3) Å^3, Z = 4, crystal dimensions: 0.28 × 0.26 × 0.22 mm^3, MoK$_\alpha$ radiation, 273 (2) K; 20464 reflections, 11201 independent, (μ = 1.407 mm^{-1}), refinement (on F^2) with SHELXTL (version 6.1), 668 parameters, 0 restraints, R_1= 0.0819 ($I > 2\sigma$) and wR_2 (all data) = 0.2517, GOF = 1.256, max/min residual electron density: 1.195/−1.473 e Å^{-3}.

Preparation of $Pd_2[(C_6H_4)PPh_2]_2[R-N-N-N-R]_2$, R = *o*-$MeC_6H_4$ (*o*-3d); R = *p*-$MeOC_6H_4$ (*p*-3c). These compounds were obtained by reaction of the potassium triazenide with the cationic $[Pd_2[(C_6H_4)PPh_2]_2(NCMe)_4][BF_4]_2$. The potassium triazenide was prepared by reaction of a CH_2Cl_2 solution (2 mL) of the triazene (0.223 mmol) with potassium hydroxide (0.223 mmol) dissolved in the minimum amount of methanol. Each solution was added to $[Pd_2[(C_6H_4)PPh_2]_2(NCMe)_4][BF_4]_2$ that was prepared by reaction of a suspension of $[Pd((C_6H_4)PPh_2)Br]_4$ (1) (100 mg, 0.056 mmol) in 20 mL of CH_2Cl_2/NCMe (8/1) with $AgBF_4$ (43 mg, 0.223 mmol). After 5 min of stirring, the solution was evaporated to dryness. The yellow crude product obtained was extracted with dichloromethane, filtered over a short plug of Celite, and precipitated by addition of hexane to give an orange-yellow microcrystalline powder, which was collected by filtration and washed with hexane. Yield: 44.0 mg (31.5%) *o*-**3d**; 84.4 mg (62%) (*p*-**3c**).

*Characterization Data for o-**3d**.* ^{1}H NMR ($CDCl_3$, 500 MHz, 298 K) δ 8.0 (m, 2H, ar), 7.53 (m, 2H, ar), 7.19 (m, 8H, ar), 7.05 (m, 16H, ar), 6.90 (m, 4H, ar), 6.82 (m, 4H, ar), 6.74 (m, 8H, ar), 1.54 (s, 6H, CH_3) 1.47 (s, 6H, CH_3); ^{31}P NMR ($CDCl_3$, 202 MHz, 298 K) δ −0.3 (s); ^{13}C NMR ($CDCl_3$, 125 MHz, 223 K) δ 163.2 (m, C metalated), 149.2 (s, C−N), 148.4 (s, C−N), 141.4−121.0 (ar), 20.8 (s, CH_3). Anal. Calcd for $C_{64}H_{56}N_6P_2Pd_2$: C, 64.93; H, 4.73; N 7.10. Found: C, 64.22; H, 4.48; N 6.91.

*X-ray Crystal Structure Data for o-**3d** (CCDC 996516).* Empirical formula: $C_{64}H_{56}N_6P_2Pd_2$, crystal system: monoclinic, space group: $P2(1)$, a = 11.358 (2) Å, b = 21.407(4) Å, c = 11.467 (2) Å, β = 105.09 (3)°, V = 2696.0 (9) Å^3, Z = 4, crystal dimensions: 0.25 × 0.23 × 0.20 mm^3, MoK$_\alpha$ radiation, 273 (2) K; 10196 reflections, 10196 independent, (μ = 0.775 mm^{-1}); refinement (on F^2) with SHELXTL (version 6.1), 667 parameters, 1 restraints, R_1= 0.0505 ($I > 2\sigma$) and wR_2 (all data) = 0.1394, GOF = 1.072, max/min residual electron density: 0.796/−0.841 e Å^{-3}.

*Characterization Data for p-**3c**.* ^{1}H NMR (CD_2Cl_2, 400 MHz, 223 K) δ 7.6 (m, 4H, ar), 7.4 (m, 2H, ar), 7.3 (m, 2H, ar), 7.2 (m, 2H, ar), 7.1 (m, 8H, ar), 7.0 (m, 8H, ar), 6.8 (m, 4H, ar), 6.7 (m, 8H, ar), 6.6 (m, 4H, ar), 6.5 (m, 2H, ar), 3.7 (s, 12H, CH_3); ^{31}P NMR (CD_2Cl_2, 162 MHz, 223 K) δ 4.4 (s); ^{13}C NMR (CD_2Cl_2, 100 MHz, 223 K) δ 163.3 (m, C metalated), 155.6 (s, C−N), 155.5 (s, C−N), 144.6−112.4 (ar), 55.3 (s, CH_3O), 55.3 (s, CH_3O). Anal. Calcd for $C_{64}H_{56}N_6O_4P_2Pd_2$: C, 61.59; H, 4.81; N 6.73. Found: C, 62.05; H, 4.32; N 6.98.

*X-ray Crystal Structure Data for p-**3c** (CCDC 996519).* Empirical formula: $C_{64}H_{56}N_6P_2Pd_2O_6$, crystal system: monoclinic, space group: $P2(1)/c$, a = 14.027 (3) Å, b = 18.857 (4) Å, c = 24.459 (5) Å, β = 105.43 (3)°, V = 6236 (2) Å^3, Z = 4, crystal dimensions: 0.24 × 0.20 × 0.18 mm^3, MoK$_\alpha$ radiation, 273 (2) K; 17083 reflections, 10200 independent, (μ = 1.363 mm^{-1}); refinement (on F^2) with SHELXTL (version 6.1), 725 parameters, 0 restraints, R_1= 0.0649 ($I > 2\sigma$) and wR_2 (all data) = 0.1731, GOF = 1.125, max/min residual electron density: 0.935/−0.610e Å^{-3}.

Synthesis of $Pd_2[(C_6H_4)PPh_2]_2[R-N-N-N-R]_2$, R = *o*-$MeOC_6H_4$ (*o*-3c). Sodium triazenide was prepared in dried THF by reaction of *o*-MeOPh-N═N-NH-*o*-MeOPh (0.223 mmol) and sodium hydride (0.223 mmol) and added to $[Pd_2[(C_6H_4)PPh_2]_2(NCMe)_4][BF_4]_2$ obtained by reaction of a suspension of $[Pd((C_6H_4)PPh_2)Br]_4$ (1) (100 mg, 0.056 mmol) in 20 mL of CH_2Cl_2/NCMe (8/1) with $AgBF_4$ (43 mg, 0.223 mmol). After 5 min of stirring, the solution was evaporated to dryness. The orange crude product obtained was extracted with dichloromethane, filtered over a short plug of silica, and precipitated by addition of hexane to give an orange microcrystalline powder, which was collected by filtration and washed with hexane. Yield: 84.4 mg (62%).

*Characterization Data for o-**3c**.* ^{1}H NMR ($CDCl_3$, 500 MHz, 298 K) δ 7.42 (m, 4H, ar), 7.34 (m, 2H, ar), 7.13 (m, 2H, ar), 7.11 (m, 4H, ar), 7.07 (m, 2H, ar), 6.95 (m, 8H, ar), 6.77 (m, 12H, ar), 6.63 (m, 8H, ar), 6.44 (m, 2H, ar), 1.47 (s,12H, CH_3); ^{31}P NMR ($CDCl_3$, 202 MHz, 298 K) δ 2.5 (s); ^{13}C NMR ($CDCl_3$, 125 MHz, 298 K) δ 165.9 (m, C metalated), 152.9 (s, C−N), 150.5 (s, C−N), 141.4−121.0 (ar), 20.8 (s, CH_3). Anal. Calcd for $C_{64}H_{56}N_6O_4P_2Pd_2$: C, 61.59; H, 4.81; N 6.73. Found: C, 61.24; H, 4.28; N 6.42.

Study by ^{31}P NMR Spectroscopy between 200 to 298 K for the Oxidation Reactions of Compounds 3a−d with $PhICl_2$. A solution of the corresponding palladium(II) compound (**3a**, *o*-**3b**−**d**, and *p*-**3b**-**d**) (0.004 mmol) in CD_2Cl_2 (0.5 mL) was cooled in a NMR tube at 200 K, and the ^{1}H and ^{31}P NMR spectra were recorded. A stoichiometric quantity of $PhICl_2$ (0.004 mmol) was added, and the color of the solution immediately changed from yellow to red. The ^{31}P NMR spectra were recorded at different temperatures from 200 to 298 K.

Synthesis of $Pd_2[(C_6H_4)PPh_2]_2[RNNNR]_2Cl_2$ R = C_6H_5 (5a); R = *p*-BrC_6H_4 (*p*-5b). To a solution at 223 K of **3a** or *p*-**3b** (0.044 mmol) in CH_2Cl_2 (5 mL) was added iodobenzene dichloride (18 mg, 0.066 mmol). The solution immediately changed from yellow to red. After 5 min of stirring, the solution was evaporated to dryness and hexane was added. The red microcrystalline precipitate obtained was isolated by filtration and washed with hexane. Yield: 40.2 mg (76%) **5a**; 44.5 mg (72%) *p*-**5b**.

*Characterization Data for **5a**.* ^{1}H NMR (CD_2Cl_2, 400 MHz, 223 K) δ 7.9 (m, 2H, ar), 7.8 (m, 2H, ar), 7.7 (m, 4H, ar), 7.5 (m, 6H, ar), 7.3 (m, 2H, ar), 7.2 (m, 4H, ar), 7.0 (m, 24H, ar), 6.8 (m, 2H, ar), 6.5 (m, 2H, ar); ^{31}P NMR (CD_2Cl_2, 162 MHz, 223 K) δ −35.6 (s); ^{13}C NMR (CD_2Cl_2, 100 MHz, 223 K) δ 154.6 (m, C metalated), 150.1 (s, C−N, trans to C), 149.3 (d, C−N, trans to P, $^3J_{P-C}$ = 5 Hz), 148.9−122−2 (ar).

*Characterization Data for p-**5b**.* ^{1}H NMR (CD_2Cl_2, 400 MHz, 223 K) δ 7.9 (m, 4H, ar), 7.8 (m, 2H, ar), 7.7 (m, 4H, ar), 7.5 (m, 4H, ar), 7.4 (m, 4H, ar), 7.1 (m, 12H, ar), 7.0 (m, 8H, ar), 6.9 (m, 4H, ar), 6.8 (m, 2H, ar); ^{31}P NMR (CD_2Cl_2, 162 MHz, 223 K) δ −34.7 (s); ^{13}C NMR (CD_2Cl_2, 100 MHz, 223 K) δ 154.4 (m, C metalated), 148.9 (s, C−N), 148.2 (s, C−N), 141.2−117.4 (ar).

Direct Catalytic Phenylation of Indole. The procedure reported by Sandford and co-workers has been followed.[13] Indole (58.6 mg, 0.5 mmol) and the precatalysts (0.0125 mmol, 2.5 mol % of Pd) were dissolved in CH_3CO_2H (5 mL) (in the case of the precatalysts *o*-**3b**, *p*-**3b**, *p*-**3c**, and *p*-**3d** a minimum volume of CH_2Cl_2 was added to dissolve), and the solution was stirred at 298 K for 5 min. $[Ph_2I]PF_6$ (426.0 mg, 1 mmol) was added, and the resulting solution stirred at 298 K until no indole was observed by ^{1}H NMR. The reaction mixture was filtered through a plug of siliceous earth and evaporated to dryness. The resulting oil was dissolved in CH_2Cl_2 (25 mL) and extracted with aqueous $NaHCO_3$ (2 × 40 mL). The organic phase was

dx.doi.org/10.1021/om500702j | *Organometallics* 2014, 33, 5378−5391

dried with Na_2SO_4, concentrated, and purified by chromatography on silica gel using as eluent hexanes/ethyl acetate (96:4).

Characterization Data for **7**. ^{1}H NMR ($CDCl_3$, 400 MHz) δ 8.31 (br s, 1H), 7.69−7.65 (m, 3H), 7.49−7.39 (m, 3H), 7.356 (t, 1H, $^3J_{H-H}$ = 7.4 Hz), 7.23 (ddd, 1H, $^3J_{H-H}$ = 7.8 Hz, $^3J_{H-H}$ = 7.0 Hz, $^3J_{H-H}$ = 1.2 Hz), 7.16 (ddd, 1H, $^3J_{H-H}$ = 7.7 Hz, $^3J_{H-H}$ = 7.0 Hz, $^3J_{H-H}$ = 1.0 Hz), 6.86 (s, 1H), ^{13}C NMR ($CDCl_3$, 100 MHz) δ 137.8 (s, C quaternary), 136.7 (s, C quaternary), 132.2 (s, C quaternary), 129.2 (s, 2 C−H), 129.0 (s, 2 C−H), 127.7 (s, C quaternary), 125.1 (s, C−H), 122.3 (s, C−H), 120.6 (s, C−H), 120.2 (s, C−H), 110.9 (s C−H), 99.9 (s, C−H).

Computational Details. All models were fully optimized with the Gaussian09 program package[25] at the DFT level of theory. A hybrid density functional B3PW91[26,27] was utilized together with the basis set consisting of the Stuttgart-Dresden effective core potential basis set with an additional p-polarization function for Pd atoms (SDD(p)) and the standard all-electron basis set 6-31G(d) for all other atoms. Frequency calculations with no scaling were performed to ensure optimization to true minima. None of the optimized structures gave imaginary frequencies.

To further study the electronic properties of the complexes, we performed topological charge density analysis with the QTAIM (Quantum Theory of Atoms in Molecules)[28] methods, which allowed us to access the nature of the bonding via calculating different properties of the electron density at the bond critical points (BCPs). The analysis was done with the AIMALL program[29] using the wave functions obtained from the DFT calculations with the computationally optimized structures.

■ ASSOCIATED CONTENT

Supporting Information

Voltammograms for compounds **3a**, *o*-**3b**, *p*-**3c**, voltammograms for *p*-bromophenyltriazene, voltammogram for compound *p*-**5b**, cyclic voltammogram for compound *p*-**3c** with TEACl, cyclic voltammogram for compound **3a** with TEACl, cyclic voltammogram for TEACl in CH_2Cl_2, cyclic voltammogram for compound *p*-**3c** with TEACl, optimized structures for *ortho*-phenyl substituted triazenide complexes *o*-**3b** and *o*-**3c**, noncovalent interactions in the crystal structure of the *o*-**3b** triazenide complex, comparison of the properties of the Pd−Pd and the axial interactions in the monophenylated complex type **3a+Ph+Cl**, selected properties of the electron density at the critical points for selected weak intramolecular interactions for Pd(II) compounds *o*-**3b**, *o*-**3c**, and *o*-**3b_dim**, selected properties of the electron density at the bond critical point for Pd(II) compounds **3a**, *o*-**3b−d**, and *o*-**3b_dim**, selected properties of the electron density at the Pd−Pd bond critical point for Pd(III) compounds **5a**, *o*-**5b−d**, and *p*-**5b-d**, the effect axial interaction of phenyl groups on the Pd−Pd and Pd−C(Ph) distances in the compounds **3a**, *o*-**3b−d**, and *p*-**3b−d**, and crystallographic data of compounds **3a**, *o*-**3b**, *o*-**3d**, *p*-**3b**, *p*-**3c**, *p*-**3d**, and *o*-**4b** in CIF format. This material is available free of charge via the Internet at http://pubs.acs.org.

■ AUTHOR INFORMATION

Corresponding Authors

*E-mail: angeles.ubeda@uv.es.

*E-mail: pipsa.hirva@uef.fi.

Notes

The authors declare no competing financial interest.

■ ACKNOWLEDGMENTS

The authors thank the Universidad de Valencia for financial support. The computational work has been facilitated by the use of the Finnish Grid Infrastructure resources. Dedicated to Professor Pascual Lahuerta on the occasion of his 70th birthday.

■ REFERENCES

(1) (a) Albertin, G.; Antoniutti, S.; Bedin, M.; Castro, J.; García-Fontán, S. *Inorg. Chem.* **2006**, *45*, 3816−3825. (b) Johnson, A. L.; Willcocks, A. M.; Richards, S. P. *Inorg. Chem.* **2009**, *48*, 8613−8622.

(2) Kimbal, D. B.; Herges, R.; Haley, M. M. *J. Am. Chem. Soc.* **2002**, *124*, 1572−1573.

(3) (a) Payehghadr, M.; Rofouei, M. K.; Morsali, A.; Shamsipur, M. *Inorg. Chim. Acta* **2007**, *360*, 1792−1798. (b) GuhaRoy, C.; Butcher, R. J.; Bhattacharya, S. *J. Organomet. Chem.* **2008**, *693*, 3923−3931. (c) Albertin, G.; Antoniutti, S.; Castro, J.; Paganelli, S. *J. Organomet. Chem.* **2010**, *695*, 2142−2152.

(4) (a) Hauber, S. O.; Lissner, F.; Deacon, G. B.; Niemeyer, M. *Angew. Chem., Int. Ed.* **2005**, *44*, 5871−5875. (b) Nuricumbo-Escobar, J. J.; Campos-Alvarado, C.; Ríos-Moreno, G.; Morales-Morales, D.; Walsh, P. J.; Parra-Hake, M. *Inorg. Chem.* **2007**, *46*, 6182−6189. (c) Litlabø, R.; Lee, H. S.; Niemeyer, M.; Törnroos, K. W.; Anwander, R. *Dalton Trans.* **2010**, *39*, 6815−6815. (d) Chu, J.; Lv, Q-y.; Xie, X-h.; Li, W.; Zhan, S. *Transition Met. Chem.* **2013**, *38*, 843−847. (e) Chu, J.; Xie, X-h.; Yang, S-r.; Zhan, S-z. *Inorg. Chim. Acta* **2014**, *410*, 191−194.

(5) Singhal, A.; Jain, V. K.; Nethaji, M.; Samuelson, A. G.; Jayaprakash, D.; Butcher, R. J. *Polyhedron* **1998**, *17*, 3531−3540.

(6) Ruis, J.; López, J. F.J.; Rodríguez, V.; Pérez, J.; Ramírez de Arellano, M. C.; López, G. *Dalton Trans.* **2001**, 2683−2689.

(7) (a) García-Herbosa, G.; Connelly, N. G.; Muñoz, A.; Cuevas, J. V.; Orpen, A. G.; Politzer, S. D. *Organometallics* **2001**, *20*, 3223−3229. (b) Cuevas, J. V.; García-Herbosa, G.; Muñoz, M. A.; Hickman, S. W.; Orpen, A. G.; Connelly, N. G. *J. Chem. Soc., Dalton Trans.* **1995**, 4127−4128. (c) Corbett, M.; Hoskins, B. F.; McLeod, N. J.; O'Day, B. P. *Aust. J. Chem.* **1975**, *28*, 2377−2392.

(8) (a) Cotton, A. F.; Koshevoy, I. O.; Lahuerta, P.; Murillo, C. A.; Sanaú, M.; Úbeda, M. A.; Zhao, Q. *J. Am. Chem. Soc.* **2006**, *128*, 13674−13679. (b) Penno, D.; Lillo, V.; Koshevoy, I. O.; Sanaú, M.; Úbeda, M. A.; Lahuerta, P.; Fernández, E. *Chem.—Eur. J.* **2008**, *14*, 10648−10655. (c) Penno, D.; Estevan, E.; Fernández, E.; Hirva, P.; Lahuerta, P.; Sanaú, M.; Úbeda, M. A. *Organometallics* **2011**, *30*, 2083−2094. (d) Ibañez, S.; Estevan, F.; Hirva, P.; Sanaú, M.; Úbeda, M. A. *Organometallics* **2012**, *31*, 8098−8108. (e) Ibañez, S.; Vrečko, D. N.; Estevan, F.; Hirva, P.; Sanaú, M.; Úbeda, M. A. *Dalton Trans.* **2014**, *43*, 2961−2970.

(9) (a) Powers, D. C.; Ritter, T. *Top. Organomet. Chem.* **2011**, *35*, 129−156. (b) Mirica, L. M.; Khusnutdinova, J. R. *Coord. Chem. Rev.* **2013**, *257*, 299−314.

(10) (a) Powers, D. C.; Ritter, T. *Nature* **2009**, *1*, 302−309. (b) Powers, D. C.; Geibel, M. A. L.; Kein, J. E. M. N.; Ritter, T. *J. Am. Chem. Soc.* **2009**, *131*, 17050−17051. (c) Chuang, G. J.; Wang, W.; Lee, E.; Ritter, T. *J. Am. Chem. Soc.* **2011**, *133*, 1760−1762. (d) Campbell, M. G.; Powers, D. C.; Raynaus, J.; Graham, M. J.; Xie, P.; Lee, E.; Ritter, T. *Nat. Chem.* **2011**, *3*, 949−953.

(11) Powers, D. C.; Ritter, T. *Organometallics* **2013**, *32*, 2042−2045.

(12) Khusnutdinova, J. R.; Rath, N. P.; Mirica, L. M. *Angew. Chem., Int. Ed.* **2011**, *50*, 5532−5536.

(13) Hickman, A. J.; Sanford, M. S. *Nature* **2012**, *484*, 177−185.

(14) (a) Powers, D. C.; Benitez, D.; Tkatchouk, E.; Goddard, W. A.; Ritter, T. *J. Am. Chem. Soc.* **2010**, *132*, 14092−14103. (b) Powers, D. C.; Xiao, D. Y.; Geibel, M. A. L.; Ritter, T. *J. Am. Chem. Soc.* **2010**, *132*, 14530−14536. (c) Powers, D. C.; Ritter, T. *Acc. Chem. Res.* **2012**, *45*, 840−850.

(15) (a) Seregin, I. V.; Gevorgyan, V. *Chem. Soc. Rev.* **2007**, *36*, 1173−1193. (b) Ackermann, L.; Vicente, R.; Kapdi, A. R. *Angew. Chem., Int. Ed.* **2009**, *48*, 9792−9826. (c) Deprez, N. R.; Kalyani, D.; Krause, A.; Sanford, M. S. *J. Am. Chem. Soc.* **2006**, *128*, 4972−4973.

(16) (a) Umakoshi, K.; Ichimura, A.; Kinoshita, I.; Ooi, S. *Inorg. Chem.* **1990**, *29*, 4005−4010. (b) Koshevoy, I. O.; Lahuerta, P.; Sanaú, M.; Úbeda, M. A.; Doménech, A. *Dalton Trans.* **2006**, 5536−5541. (c) Durrell, A. C.; Jackson, M. N.; Hazari, N.; Gray, H. B. *Eur. J. Inorg. Chem.* **2013**, 1134−1137.

(17) (a) Besenyei, G.; Párkányi, L.; Gács-Baitz, E.; James, B. R. *Inorg. Chim. Acta* **2002**, *327*, 179−187. (b) Ogura, T.; Yoshida, K.; Yanagisawa, A.; Imamoto, T. *Org. Lett.* **2009**, *11*, 2245−2248. (c) Ganesamoorthy, C.; Mague, J. T.; Balakrishna, M. *J. Organomet. Chem.* **2007**, *692*, 3400−3408. (d) Brub, J.-F.; Gagnon, K.; Fortin, D.; Decken, A.; Harvey, P. H. *Inorg. Chem.* **2006**, *45*, 2812−2823.
(18) Bonet, A.; Gulyás, H.; Koshevoy, I. O.; Estevan, F.; Sanaú, M.; Úbeda, M. A.; Fernández, E. *Chem.—Eur. J.* **2010**, *16*, 6382−6390.
(19) Davidson, D. V.; Garg, S. K. *Can. J. Chem.* **1972**, *50*, 3515−3520.
(20) Canty, A. J.; Ariafard, A.; Sanford, M. S.; Yates, B. F. *Organometallics* **2013**, *32*, 544−555.
(21) (a) Estevan, F.; García-Bernabé, A.; Lahuerta, P.; Sanaú, M.; Úbeda, M. A.; Ramirez de Arellano, M. C. *Inorg. Chem.* **2000**, *39*, 5964−5969. (b) Aarif, A. M.; Estevan, F.; García-Bernabé, A.; Lahuerta, P.; Sanaú, M.; Úbeda, M. A. *Inorg. Chem.* **1997**, *36*, 6472−6475.
(22) Lucas, H. J.; Kennedy, E. R. *Organic Synthesis*; Wiley & Sons: New York, 1955; Collect. Vol. *III*, p 482.
(23) Hartmann, W. W.; Dickey, J. B. *Org. Synth.* **1943**, *2*, 163−165.
(24) *SHELXTL* (Version 6;14); Brucker: 2000.
(25) Frisch, M. J.; Trucks, G. W.; Schlegel, H. B.; Scuseria, G. E.; Robb, M. A.; Cheeseman, J. R.; Scalmani, G.; Barone, V.; Mennucci, B.; Petersson, G. A.; Nakatsuji, H.; Caricato, M.; Li, X.; Hratchian, H. P.; Izmaylov, A. F.; Bloino, J.; Zheng, G.; Sonnenberg, J. L.; Hada, M.; Ehara, M.; Toyota, K.; Fukuda, R.; Hasegawa, J.; Ishida, M.; Nakajima, T.; Honda, Y.; Kitao, O.; Nakai, H.; Vreven, T.; Montgomery, J. A., Jr.; Peralta, J. E.; Ogliaro, F.; Bearpark, M.; Heyd, J. J.; Brothers, E.; Kudin, K. N.; Staroverov, V. N.; Kobayashi, R.; Normand, J.; Raghavachari, K.; Rendell, A.; Burant, J. C.; Iyengar, S. S.; Tomasi, J.; Cossi, M.; Rega, N.; Millam, J. M.; Klene, M.; Knox, J. E.; Cross, J. B.; Bakken, V.; Adamo, C.; Jaramillo, J.; Gomperts, R.; Stratmann, R. E.; Yazyev, O.; Austin, A. J.; Cammi, R.; Pomelli, C.; Ochterski, J. W.; Martin, R. L.; Morokuma, K.; Zakrzewski, V. G.; Voth, G. A.; Salvador, P.; Dannenberg, J. J.; Dapprich, S.; Daniels, A. D.; Farkas, Ö.; Foresman, J. B.; Ortiz, J. V.; Cioslowski, J. J.; Fox, D. J. *Gaussian 09, Revision C.01*; Gaussian, Inc.: Wallingford, CT, 2009.
(26) Becke, A. D. J. *Chem. Phys.* **1993**, *98*, 5648−5652.
(27) Perdew, J. P.; Wang, Y. *Phys. Rev. B* **1992**, *45*, 13244−13249.
(28) Bader, R. F. W. In *Atoms in Molecules: A Quantum Theory*; Clarendon Press: Oxford, 1990.
(29) Keith, T. A. *AIMAll* (Version 12.06.03); TK Gristmill Software: Overland Park, KS, USA, 2012 (aim.tkgristmill.com).